TPB

Spatial Structure, Environmental Heterogeneity, and Population Dynamics: Analysis of the Coupled Logistic Map

Bruce E. Kendall*

*Department of Ecology and Evolutionary Biology, University of Arizona, Tucson,
Arizona 85721, and National Center for Ecological Analysis and Synthesis,
University of California, Santa Barbara, California 93106*

and

Gordon A. Fox[†]

*Department of Biology 0116, University of California San Diego, 9500 Gilman Drive, La Jolla,
California 92093-0116, and Department of Biology, San Diego State University,
San Diego, California 92182*

Spatial extent can have two important consequences for population dynamics: It can generate *spatial structure*, in which individuals interact more intensely with neighbors than with more distant conspecifics, and it allows for *environmental heterogeneity*, in which habitat quality varies spatially. Studies of these features are difficult to interpret because the models are complex and sometimes idiosyncratic. Here we analyze one of the simplest possible spatial population models, to understand the mathematical basis for the observed patterns: two patches coupled by dispersal, with dynamics in each patch governed by the logistic map. With suitable choices of parameters, this model can represent spatial structure, environmental heterogeneity, or both in combination. We synthesize previous work and new analyses on this model, with two goals: to provide a comprehensive baseline to aid our understanding of more complex spatial models, and to generate predictions about the effects of spatial structure and environmental heterogeneity on population dynamics.

Spatial structure alone can generate positive, negative, or zero spatial correlations between patches when dispersal rates are high, medium, or low relative to the complexity of the local dynamics. It can also lead to quasiperiodicity and hyperchaos, which are not present in the nonspatial model. With density-independent dispersal, spatial structure cannot destabilize equilibria or periodic orbits that would be stable in the absence of space. When densities in the two patches are uncorrelated, the probability that the population in a patch reaches extreme low densities is reduced relative to the same patch in isolation; this ''rescue effect'' would reduce the probability of metapopulation extinction beyond the simple effect of spreading of risk.

* E-mail: kendall@nceas.ucsb.edu. Fax: (805) 892-2510. Present address: National Center for Ecological Analysis and Synthesis, University of California, Santa Barbara, California 93106.
† E-mail: gfox@ucsd.edu.

Pure environmental heterogeneity always produces positive spatial correlations. The dynamics of the entire population is approximated by a nonspatial model with mean patch characteristics. This approximation worsens as the difference between the patches increases and the dispersal rate decreases: Under extreme conditions, destabilization of equilibria and periodic orbits occurs at mean parameter values lower than those predicted by the mean parameters. Apparent within-patch dynamics are distorted: The local population appears to have the wrong growth parameter and a constant number of immigrants (or emigrants) per generation.

Adding environmental heterogeneity to spatial structure increases the occurrence of spatially correlated population dynamics, but the resulting temporal dynamics are more complex than would be predicted by the mean parameter values. The three classes of spatial pattern (positive, negative, and zero correlation), while still mathematically distinct, become increasingly similar phenomenologically.   © 1998 Academic Press

1. INTRODUCTION

The individuals comprising a population are distributed in space. This has two potentially important consequences for population dynamics: There may be spatial population structure (individuals interact more frequently with neighbors than with more distant individuals), and there may be environmental heterogeneity (individuals at different locations experience different environments, and thus different birth and death rates). Spatial structure is frequently invoked to explain competitive coexistence (Levin,1974; Iwasa and Roughgarden, 1986; Kishimoto, 1990; Nee and May, 1992), the persistence of predator–prey and host–parasitoid interactions (Huffaker, 1958; Allen, 1975; Hilborn, 1975; Gurney and Nisbet, 1978; Fujita, 1983; Nachman, 1987; Reeve, 1988; Sabelis and Diekmann, 1988; Comins *et al.*, 1992), and the regional persistence of small populations subject to local stochastic extinction (den Boer, 1981; Day and Possingham, 1995). Spatial structure is also the dominant feature of meta-population models (reviewed in Gilpin and Hanski, 1991; Hanski and Gilpin, 1997). Environmental hetero-geneity has most frequently been studied in the context of source-sink dynamics (Pulliam, 1988; Pulliam, 1996).

There are many important questions about these effects of spatial extent. What causes synchrony (or asynchrony) between populations at various locations? Does spatial structure stabilize (or destabilize) population dynamics? Could the population persist in the absence of spatial structure? Given that a population is spatially structured, at what level of detail do we need to sample it in order to understand the underlying processes? These questions, and others like them, are difficult to answer empirically, because they require population data of large spatial and temporal extent, tied to information about dispersal (but see Hanski and Woiwood, 1993; Holyoak and Lawler,

1996; Sutcliffe *et al.*, 1996). Thus we we must turn to theory for guidance.

The spatial component of population dynamics has inspired a variety of modeling formalisms, which differ in grain and detail. Space, time, and local population state may be treated as discrete or continuous variables. Local population processes and explicit spatial locations may or may not be explicitly modeled. For example, a coupled map lattice is discrete in time and space, has a continuous range of local densities, has nonlinear local population dynamics, and usually includes explicit space (Comins *et al.*, 1992; Allen *et al.*, 1993; Doebeli, 1995; Rohani and Miramontes, 1995; Comins and Hassell, 1996; Ruxton and Doebeli, 1996; Heino *et al.*, 1997). In these models episodes of within-patch reproduction and survival (which may involve multiple species) alternate with dispersal among patches. This formalism can be used to examine both population structure, by letting the dispersal rate be small, and spatial heterogeneity, by letting the birth and death parameters vary among patches.

Coupled map lattices are capable of generating complex spatial patterns, even when the environment is identical across patches (Comins *et al.*, 1992; Ruxton and Doebeli, 1996; Ruxton and Rohani, 1996), and are used in physics to study spatio-temporal chaos (reviewed in Kaneko, 1993). If dispersal is density-independent and there is either a single species without age-structure or there are two competing species, then an equilibrium that is stable in the absence of spatial structure cannot be destabilized by spatial structure (Rohani *et al.*, 1996). There have been few additional generalizations, however: Most studies of coupled map lattices are dominated by phenomenological descriptions of the observed dynamics. We need to understand the underlying mathematical processes in these models, so that we can develop insight into which phenomena are general. One approach to this

problem starts with the simplest models that combine nonlinear population dynamics and spatial structure, and develops a thorough mathematical understanding of these models. These simple models can serve as building blocks for more complex models, and the insights gained from them can aid our understanding of the complex models.

In this paper we present such an analysis for a model with two patches linked by density-independent dispersal, with single-species dynamics within each patch given by a simple one-dimensional nonlinear model. This model can be used to look at spatial population structure and spatial environmental heterogeneity, both separately and together. This model has been studied previously (Gyllenberg *et al.*, 1993; Hastings, 1993; Lloyd, 1995); we combine those results (mostly pertaining to spatial structure) with many new ones to develop a broad synthesis of the model. This mathematical synthesis is our primary objective in this paper, but we also point out some biologically interesting insights gained along the way. We describe the model in Section 2, and in Sections 3–5 we detail the analyses relevant to spatial structure alone, environmental heterogeneity alone, and both in combination. Mathematical propositions and their proofs are in Appendix A. In Appendix B we review published analyses of closely related models, mostly from the physics literature, to assess which of our results might be mathematically robust. At times our analysis is quite technical and assumes some knowledge of nonlinear dynamics (see, for example, Thompson and Stewart, 1986; Baker and Gollub, 1996). For those wanting a general overview of our results, we suggest reading Section 2, the concluding subsections of Sections 3–5, and the Discussion (Section 6).

2. MODEL FORMULATION

Within-patch dynamics are governed by the logistic map:

$$x_i' = f(x_i) = r_i x_i (1 - x_i) \qquad (1)$$

(i indexes the patch identity; the prime denotes the succeeding generation). The variable x_i represents local density in patch i; its maximum value is one. The dynamics of this map are well understood (May, 1976). If the growth rate parameter r_i is between 0 and 1, the equilibrium at $x_i = 0$ is stable. If $1 < r_i < 3$ the equilibrium at $x_i = 1 - 1/r_i$ is stable. At $r_i = 3$ there is a period-doubling bifurcation, starting a period-doubling cascade that leads

to the onset of chaos at $r_i \approx 3.57$. If $r_i > 4$ the map generates negative numbers and is no longer interpretable as an ecological model.

We use density-independent dispersal to couple the patches: in each time step a constant fraction of each local population moves to the other patch. We assume that the dispersal rate is an intrinsic property of the organism, so the fraction leaving the natal patch is independent of patch quality. Dispersal and local interactions must happen in sequence (or else confounding effects result when individuals contribute to density-dependence in their natal patch after emigrating; Hassell *et al.*, 1995); we measure the population after dispersal but before the next round of local interactions.

The complete model is

$$
\begin{aligned}
x_1' &= (1 - D)\, r_1 x_1 (1 - x_1) + D r_2 x_2 (1 - x_2) \\
x_2' &= (1 - D)\, r_2 x_2 (1 - x_2) + D r_1 x_1 (1 - x_1),
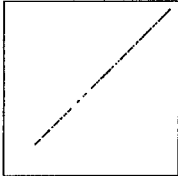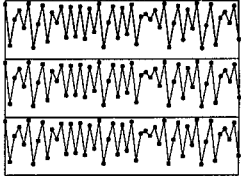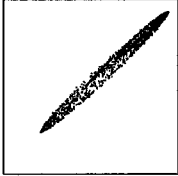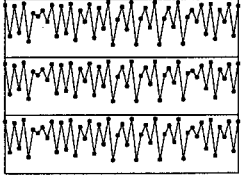\end{aligned}
\qquad (2)
$$
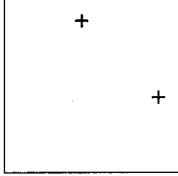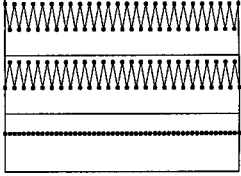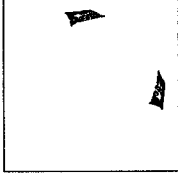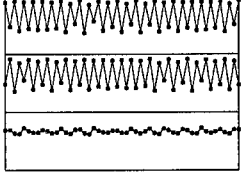
where x_1 and x_2 are the population densities (scaled from zero to one) in the two patches, r_1 and r_2 are the growth rate parameters in the two patches, and D is the dispersal rate. As we describe in the analyses that follow, the majority of the non-equilibrium dynamics generated by Eq. (2) can be grouped into six qualitative classes of spatial pattern, which we define and illustrate in Table 1.

Most previous analysis of the model has focused on spatial structure ($r_1 = r_2$; Section 3). Yamada and Fujisaka (1983) and Lloyd (1995) describe the stability criterion for the strictly in-phase orbits, and Gyllenberg *et al.* (1993) and Hastings (1993) give the positions and stability of the various equilibria 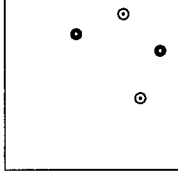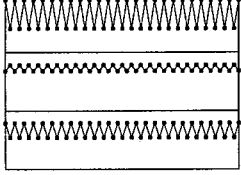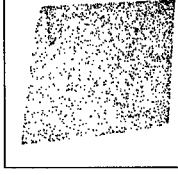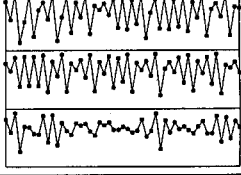and period-2 orbits. Lloyd (1995) gave qualitative descriptions of the various complex attractors. However, aside from the Naimark bifurcation (the discrete-time analog of the Hopf bifurcation, in which the eigenvalues are complex) that destabilizes the out-of-phase two-cycle, the types of bifurcations associated with these stability changes have not been described. When there are multiple coexisting attractors, the basin boundaries form a sort of "fractal checkerboard," with ever smaller blocks towards the edges of the unit square (Gyllenberg *et al.*, 1993; Hastings, 1993). This fractal pattern is destroyed by only small amounts of noise (Hastings, 1993).

There are many fewer results for environmental heterogeneity (Sections 4 and 5). Gyllenberg *et al.* (1993) numerically determined the parameter values for which the equilibria and two-cycles are stable. When dispersal (D) is large, the two populations tend to be nearly in phase, whereas for weaker coupling ($D \approx 0.1$) the two populations can be substantially uncorrelated (Hastings, 1993).

TABLE 1

Qualitative Classes of Non-Equilibrium Dynamics Generated by the Coupled Logistic Map. The Axes of the Phase Portraits are x_1 and x_2, Running from 0 to 1; the Time Series Are x_1, x_2, and $\bar{x} = (x_1 + x_2)/2$

Class	Definition	Typical phase portrait	Typical time series
Strictly in-phase	$x_1(n) = x_2(n)$ for all n		
Approximately in-phase	$x_1(n) \approx a x_2(n)$ for all n and some $a > 0$		
Strictly out-of-phase	$x_1(n) = x_2(n + p/2)$ and $x_2(n) = x_1(n + p/2)$ for all n, where the period p is even		
Approximately out-of-phase	$x_1(n) \approx a x_2(n + p/2)$ and $x_2(n) \approx a x_1(n + p/2)$ for all n and some $a > 0$, where the period p is even		
Anti-phase[a]	Pair of orbits, $P1$ and $P2$: for each $\big(x_1(n), x_2(n)\big)$ in $P1$ there is a $\big(y_1(m), y_2(m)\big)$ in $P2$ satisfying $x_1(n) = y_2(m)$ and $x_2(n) = y_1(m)$, and vice versa		
Uncorrelated	No obvious relationship between x_1 and x_2		

[a] The phase portrait shows both anti-phase orbits; the time series is of the one in solid circles.

The next three sections detail the analysis of the coupled logistic map.

3. SPATIAL STRUCTURE ALONE

We model spatial spatial structure with low dispersal and identical growth rates in the two patches. "Low dispersal" means $D < 0.25$: less than a quarter of the local population emigrates. As we show below, this is the highest dispersal rate that allows asynchronous attractors.

All of the major classes of dynamics (Table 1) can be found under spatial structure. The strictly in-phase, or synchronous, dynamics are identical to the dynamics in the absence of space. The predominant out-of-phase dynamics are organized around a period-two cycle, which follows the torus route to chaos. When neither the in-phase nor the out-of-phase dynamics are stable, the attractors are either approximately in-phase or uncorrelated, depending on the presence or absence of the unstable out-of-phase periodic orbits.

The equations describing the equilibria, two-cycles, and major bifurcations are collected in Tables 2 and 3. Spatial structure is the most-studied aspect of the coupled logistic map; we indicate where appropriate the source of qualitative and quantitative insights. In this section we add some new quantitative results, which are mostly detailed in Table 3 and proved in Appendix A; but our major contribution is the collection of qualitative insights that show the relationships among the various sorts of dynamics (Section 3.5).

3.1. Strictly In-Phase Dynamics

If the two subpopulations start with identical densities, then in each patch, the number of immigrants exactly balances the number of emigrants. Thus the dynamics in each patch proceed as if there were no spatial structure, and the two subpopulations will remain synchronized indefinitely. These dynamics proceed on the line $x_1 = x_2$ (the "diagonal"); this line is an invariant manifold, meaning that any population starting on it remains on it. The diagonal need not be locally attracting, however.

TABLE 2

Fixed Points and Two-Cycles of the Coupled Logistic Map under Conditions of Spatial Structure Alone

Orbit	Location	
Fixed points	$(0, 0)$;	(II.1)
	$(1 - 1/r, 1 - 1/r)$	(II.2)
Strictly in-phase two-cycle	$(x, x) : x = \dfrac{r + 1 \pm \sqrt{(r + 1)(r - 3)}}{2r}$	(II.3)
Strictly out-of-phase two-cycle	$\left(\dfrac{u + v + 1}{2}, \dfrac{u - v + 1}{2} \right):$	
	$u = \dfrac{1}{r(1 - 2D)},$	
	$v = \pm \dfrac{\sqrt{[r(1 - 2D) + 1][(r - 2)(1 - 2D) - 1]}}{r(1 - 2D)}$	(II.4)
Anti-phase two-cycles	$\left(\dfrac{u + v + 1}{2}, \dfrac{u - v + 1}{2} \right):$	
	$u^2 = \dfrac{1}{2r^2(1 - 2D)^2} \left[r(r - 2)(1 - 2D)^2 - 1 \pm \sqrt{[r(r - 2)(1 - 2D)^2 - 3][r(r - 2)(1 - 2D)^2 + 1]} \right]$	(II.5)
	$v^2 = 1 - u^2 - \dfrac{2}{r} - \dfrac{2}{r^3(1 - 2D)^2 u}$	

Note. These are all described by Gyllenberg *et al.* (1993).

TABLE 3

Bifurcations of the Coupled Logistic Map under Conditions of Spatial Structure Alone

Bifurcation	Criterion		Comments and sources
Non-spatial period-doubling of equilibrium (II.2)	$r = 3$	(III.1)	Same as non-spatial logistic map
Spatial period-doubling of equilibrium (II.2)	$r = 2 + \dfrac{1}{1 - 2D}$	(III.2)	Gyllenberg *et al.* (1993),[a] Proposition 4; gives rise to strictly out-of-phase two-cycle (II.4)
Local stability boundary of strictly in-phase dynamics	$D = \dfrac{1}{2}\left(1 - e^{-\varLambda_r}\right)$	(III.3)	Yamada and Fujisaka (1983) and Lloyd (1995); proof elaborated in Proposition 1. $\varLambda_r$ is the Lyapunov exponent of the non-spatial logistic map with parameter r
Pitchfork bifurcation of strictly out-of-phase two-cycle (II.4)	$r = 1 + \sqrt{1 + \dfrac{3}{(1 - 2D)^2}}$	(III.4)	Gyllenberg *et al.* (1993),[a] Lloyd (1995);[b] this stabilizes the strictly out-of-phase two-cycle (II.4) and gives rise to the pair of anti-phase two-cycles (II.5)
Eigenvalues of strictly out-of-phase two-cycle (II.4) become complex	$r = 1 + \sqrt{1 + \dfrac{(2 - 3D)^2}{(1 - 2D)^3}}$	(III.5)	New result: Proposition 5
Naimark bifurcation of strictly out-of-phase two-cycle (II.4)	$r = 1 + \sqrt{1 + \dfrac{3}{1 - 2D} + \dfrac{2}{(1 - 2D)^2}}$	(III.6)	Gyllenberg *et al.* (1993)
"Period-two" out-of-phase orbits become chaotic	$r \approx 1 + \sqrt{9.61 - \dfrac{9.71}{1 - 2D} + \dfrac{7.19}{(1 - 2D)^2}}$	(III.7)	New result: numerical approximation

[a] Gyllenberg *et al.* (1993) demonstrate the stability boundary but do not identify the bifurcation type.
[b] Lloyd (1995) identifies the bifurcation type.

If the subpopulations start with similar, but not identical, densities, then they become synchronized if the strictly in-phase dynamics are locally stable (Eq. (III.3), Fig. 1). The stability criterion relates the complexity of the non-spatial dynamics, represented by the Lyapunov exponent of f, and the level of dispersal (Yamada and Fujisaka, 1983; Lloyd, 1995; these proofs overlook some subtleties, which we address in Proposition 1). The more complex the non-spatial dynamics, the more dispersal is needed to synchronize the populations.

If in the absence of space the attractor would be periodic or equilibrial, then the synchronous dynamics are locally stable for any amount of dispersal (Lloyd 1995). Thus, spatially induced instability can only occur when the local dynamics are chaotic, and dispersal is not too large. These strictly in-phase periodic orbits need not be globally stable, however, and often coexist with out-of-phase attractors.

If the strictly in-phase dynamics are chaotic, then even if the local stability criterion is satisfied, the trajectory will sometimes move away from synchrony for short periods.

This occurs because the magnitude of expansion and contraction varies over a chaotic attractor; but it reveals that this stability, while 'local' with respect to the in-phase dynamics, is fundamentally different from the local stability of equilibria and cycles (near a stable equilibrium, for example, a trajectory moves monotonically towards the attractor).

We will revisit the stability of the strictly in-phase dynamics in Section 3.4, after examining the other classes of dynamics.

3.2. Out-of-Phase Dynamics

The predominant out-of-phase dynamics are centered around a period-two cycle (Eq. (II.4)). This two-cycle appears from a spatially-induced period doubling of the spatially symmetric equilibrium. It is a saddle when it first appears; it gains stability through a pitchfork bifurcation, and then follows the torus route to chaos. We describe this sequence in detail, and then briefly discuss the higher order out-of-phase orbits.
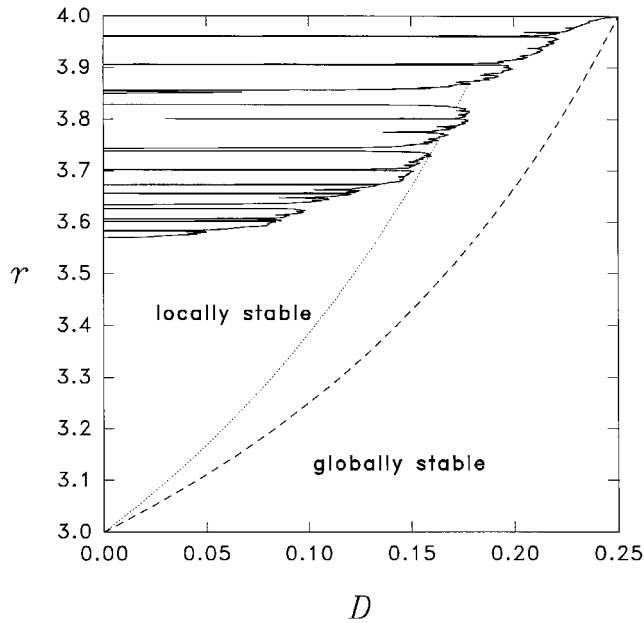
FIG. 1. Bifurcations of strictly in-phase dynamics. Solid line: local stability criterion (Eq. (III.3)); strictly in-phase dynamics are stable to the right of the curve and unstable to the left. Dashed line: Gyllenberg *et al.*'s (1993) conjectured global stability criterion. Dotted line: transition of the out-of-phase two-cycle from a saddle to a stable node. The strictly in-phase dynamics are globally attracting in much of the region between the dotted and dashed lines (Section 3.5).
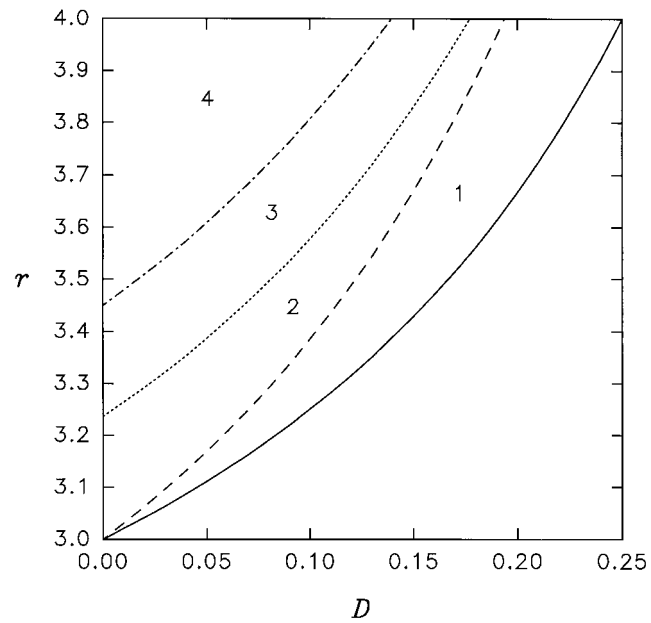
FIG. 2. Bifurcations of the strictly out-of-phase two-cycle. Solid line: the orbit appears via a period-doubling bifurcation from the equilibrium. Dashed line: the orbit becomes stable via a pitchfork bifurcation. Dotted line: the eigenvalues of the orbit become complex. Dashed-dotted line: the orbit is destabilized via a Naimark bifurcation. The orbit is a saddle in region 1, a stable node in region 2, a stable focus in region 3, and an unstable focus in region 4.

3.2.1. *Out-of-phase periodic orbits.* There are two ways to understand the appearance of the out-of-phase two-cycle. The first, described eloquently by Lloyd (1995), is to imagine the system without dispersal. If the local dynamics are a two-cycle, then the two subpopulations may be, depending on starting conditions, oscillating either in or out of synchrony with each other; the local densities attained are the same in either case. A small amount of dispersal does not change the qualitative pattern. The local densities in the out-of-phase cycle are slightly different, however, and the basins of attraction of the two attractors are somewhat deformed.

The second way of understanding the out-of-phase dynamics is to fix the dispersal and vary r (Fig. 8). When the spatially homogeneous equilibrium (Eq. (II.2)) period-doubles to produce the in-phase two-cycle (Eq. (II.3)), which is locally stable, the equilibrium is left as a saddle (Gyllenberg *et al.*,1993): it is still attracting in the off-diagonal direction. At a higher value of r the equilibrium period-doubles again (Eq. (III.2), Proposition 4), in the off-diagonal direction, producing the out-of-phase two-cycle (Eq. (II.4)). This two-cycle is itself a saddle, as it inherits the along-diagonal instability of the equilibrium.

The strictly out-of-phase two-cycle goes through several stability changes as r is increased (Table 3; Fig. 2). The first is a pitchfork bifurcation (Eq. (III.4)): the larger eigenvalue passes through $+1$, and the out-of-phase two-cycle becomes a stable node. The values of the two eigenvalues converge with further increases in r; upon becoming identical they become a complex conjugate pair (Eq. (III.5)), and the two-cycle becomes a stable focus, with trajectories spiraling in towards the attractor. When $D = 0$, this corresponds to the point where the eigenvalue of the non-spatial two-cycle changes from positive to negative. The magnitudes of the complex eigenvalues increase with r; when they pass through $+1$, the two-cycle goes through a Naimark bifurcation (Eq. (III.6)) and becomes an unstable focus.

A pair of anti-phase two-cycles (Eq. (II.5)) is produced at the pitchfork bifurcation (Gyllenberg *et al.*, 1993). When $D = 0$, this represents one subpopulation following the two-cycle and the other balanced at the unstable equilibrium. There are two such orbits, depending on which subpopulation is following the two-cycle. The orbits are saddles when they first appear; as r increases, the stable eigenvector goes through a period-doubling

bifurcation, causing the two-cycles to become unstable nodes and producing an anti-phase pair of saddle four-cycles. Numerical investigations show that the stable manifolds (the nonlinear extensions of the stable eigenvectors) of the saddle anti-phase two-cycles form the boundaries between the basins of attraction of the in-phase and out-of-phase attractors, which is a kind of "fractal checkerboard," (see figures in Gyllenberg *et al.*, 1993; Hastings, 1993; Lloyd, 1995). This boundary remains after the anti-phase two-cycles have become sources (and hence do not have stable manifolds); we suspect that they are maintained by the stable manifolds of the saddle anti-phase four-cycles (and the higher-order orbits that follow them up the period-doubling chain).

3.2.2. Out-of-phase invariant loops. When the out-of-phase two-cycle is destabilized by the Naimark bifurcation, the new attractor is a two-piece invariant loop that surrounds the two-cycle (see Figs. 7 and 11 in Lloyd, 1995). This quasiperiodic attractor is topologically conjugate to the canonical circle map. Along Eq. (III.6), the rotation number (the average angular fraction of the loop traversed per iterate) decreases monotonically from $1/2$ at $D = 0$ to about $11/25$ at $r = 4$ (Proposition 6). The rational values of the rotation number correspond to periodic orbits on the loop; these expand into "locking regions" of periodic orbits with nonzero width above the Naimark bifurcation. Each locking region contains an anti-phase pair of stable periodic orbits, and a corresponding anti-phase pair of periodic saddles separating them.

The only locking region that covers a substantial region of parameter space is the "strong resonance" at low values of D. There are a pair of stable four-cycles in this region. At $D = 0$ these are simply two of the four combinations of unlinked four-cycles (Lloyd, 1995). Between them on the invariant loop is an anti-phase pair of saddle four-cycles; when $D = 0$ these correspond to one patch following the four-cycle and the other following the unstable two-cycle. As r increases the range of D-values for which these anti-phase four-cycles exist increases.

3.2.3. Out-of-phase chaotic dynamics. In the strong resonance region, the out-of-phase attractors follow the period-doubling route to chaos as r increases. This route is somewhat unusual, however, in that each period-doubling bifurcation produces an anti-phase pair of new orbits, and the saddles also period-double. Thus there are n distinct out-of-phase $2 \times n$-cycles and an equal number of saddles separating them. After the accumulation point, as the chaotic bands merge with each other in the reverse of the period-doubling cascade, they also merge with the other members of the relevant pair, resulting in a $2 \times n$-piece chaotic attractor, with each piece approximately

square (Fig. 3). Each band-merging is a crisis (Grebogi *et al.*, 1983), caused, we suspect, by a collision of the attractors with a stable manifold of the saddle chaotic orbits separating the anti-phase pair of attractors. Immediately beyond the crisis, the pairs of chaotic structures nearly maintain their separate identity: the trajectory only occasionally switches from one to the other. Further increases in r cause the pieces to merge, and their "folded" structure knits together seamlessly (Fig. 3).

The remainder of the invariant loop broadly follows the torus route to chaos with increasing r. The transition is complicated, as there are many coexisting attractors, and each locking region has its own transitions to chaos. The analogy with the circle map breaks down: there

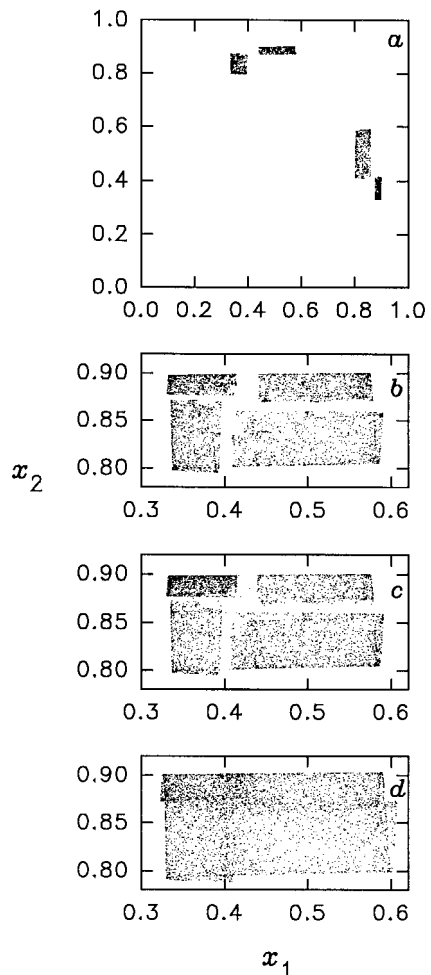**FIG. 3.** Band merging in the out-of-phase chaotic attractor. (a) The four-piece attractor: $r = 3.6132$, $D = 0.01$. (b) Magnification of the upper portion of (a), showing the coexisting anti-phase orbit. (c) Just past the crisis: $r = 3.613665$, $D = 0.01$. A single orbit is plotted, but transitions between the members of the former anti-phase pair are infrequent. (d) Complete band-merging: $r = 3.625$, $D = 0.01$.

are bifurcations of the periodic orbits, such as Naimark bifurcations, that are not found in the circle map. Outside of the locking regions, however, there is a fairly distinct transition from quasiperiodicity to chaos. The quasi-periodic invariant loop is deeply folded, and the multi-part chaotic attractor follows the general outline of the previously existing invariant loop. Further increases in r cause the parts of the attractor to expand until each of the two pieces of the attractor is filled with points (Table 1).

We determined the approximate condition for the transition to two-chaos numerically (Eq. (III.7)). The two-part chaotic attractor has each piece centered on one of the points of the unstable strictly out-of-phase periodic orbit; the trajectory hops back and forth between the two. Each piece is a simply bounded region that is completely covered by points; but the density of points varies within the attractor.

The points on the out-of-phase chaotic orbit appear to fill a region of the state space, albeit with variation in density. This resembles hyperchaos (Rössler, 1979; Baier and Klein, 1990), in which there is folding in two or more directions. Kaneko (1983) makes a similar observation, claiming that some of the attractors in his version of the coupled logistic map were hyperchaotic because they had two positive Lyapunov exponents. In invertible maps hyperchaos requires at least three state variables (Klein and Baier, 1991). The coupled logistic map, however, is is not invertible. The closest invertible analog would have four state variables, so hyperchaos (or something very similar) seems plausible in the coupled logistic map.

Further increases of r lead eventually to the destabilization of the out-of-phase chaotic orbit via a crisis. Lloyd (1995) notes that when $D = 0$ this is caused by a collision between the out-of-phase attractor and the unstable equilibrium. With dispersal it is more complex. We conjecture that the collision is with a stable manifold of the anti-phase chaotic saddle derived, via a period-doubling cascade, from the anti-phase two-cycles.

3.2.4. *Higher order out-of-phase orbits.* Arguments exactly analogous to those for the equilibrium reveal that every stable in-phase periodic orbit eventually produces an out-of-phase periodic orbit via a spatial period-doubling. This spatial period-doubling always occurs at a higher value of r than the non-spatial period-doubling. Every such out-of-phase orbit goes through a sequence of bifurcations and associated dynamics that is identical to that described above for the out-of-phase two-cycle. The associated attractors are small, as are their basins of attraction. The one exception is the out-of-phase four-cycle, which, when r is large, retains stability to a slightly larger value of D than does the out-of-phase two-cycle; it appears to be the only out-of-phase attractor in this region.

The scaling of these bifurcation sequences is not completely clear, but we can make some observations. First, the curve along which the out-of-phase orbit arises, as well as that along which it gains stability (Eqs. (III.2) and (III.4) for the two-cycle), must intersect the r-axis at the value of r corresponding to that period-doubling in the logistic map. In addition, all of the curves along which the orbits arise pass through $r = 4$, $D = 0.25$, and they do not intersect one another (Proposition 7). As we discovered numerically for the four-cycle, the curves of the pitchfork bifurcations can cross one another.

The tangent bifurcations that open the periodic windows of the in-phase dynamics also give rise to sets of anti-phase orbits. Consider the three-cycle that appears via a tangent bifurcation at $r \approx 3.83$. If $D = 0$, then three separate saddle-node pairs of three-cycles are formed at the tangent bifurcation: strictly in-phase, x_1 follows x_2, and x_1 leads x_2. For positive D, we suspect that the tangent bifurcations give rise to a saddle-node pair in which the node is unstable; the saddle is then stabilized by a pitchfork bifurcation (Fig. 4).

3.3. Uncorrelated Dynamics

When r is large and D is small then neither the in-phase nor out-of-phase dynamics are attracting. The resulting "uncorrelated" attractor (which is truly uncorrelated only when $D = 0$) contains all of the unstable out-of-phase periodic orbits, and the out-of-phase chaotic topologies
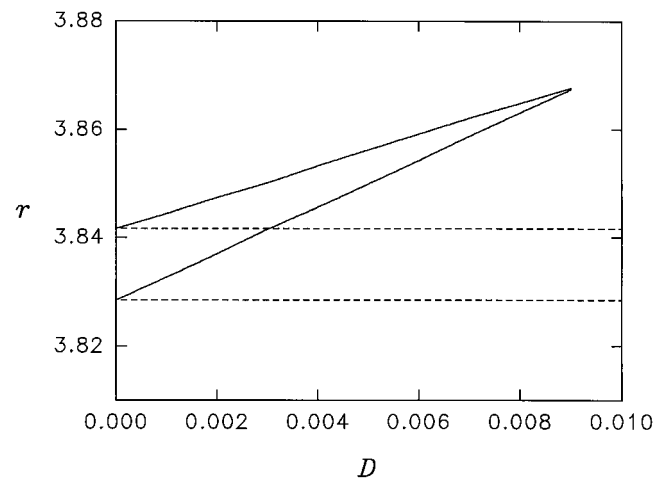

FIG. 4. Stability regions of the in-phase (dashed lines) and out-of-phase (solid lines) three-cycles. The lower boundary of each is a saddle-node bifurcation, while the upper is a period-doubling bifurcation. The stability region of the in-phase three-cycle continues unchanged for larger D.
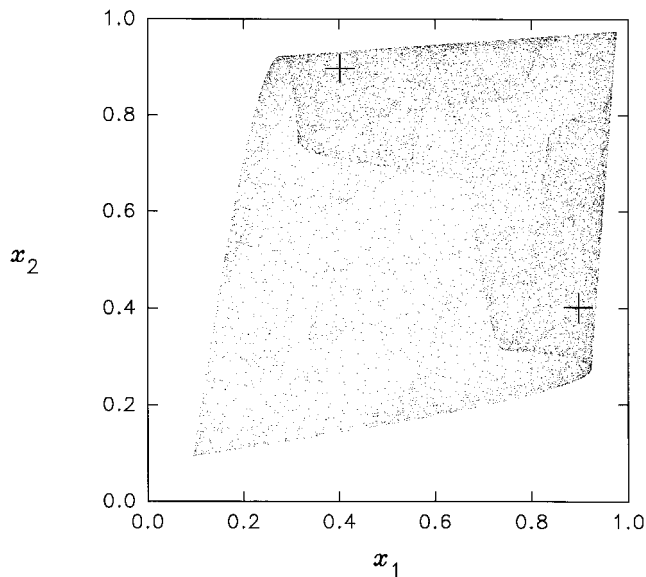
FIG. 5. An uncorrelated chaotic attractor. $r = 3.9$; $D = 0.07$. The unstable strictly out-of-phase two-cycle is indicated by $+$.

Fig. 6. The probability of finding a local population (x_1) at a given size, calculated by iterating the model for 50 000 generations and counting how many times (x_1) falls within one of 200 bins between zero and one. (a) No dispersal: $r = 3.95$, $D = 0$. (b) Low dispersal, leading to uncorrelated dynamics: $r = 3.95$, $D = 0.07$.

associated with them (Fig. 5). This causes transient periodicity (Kendall *et al.*, 1993), in which the trajectory spends extended periods trapped in the unstable manifolds of the unstable periodic orbit, showing episodes of nearly periodic dynamics (in this case, out-of-phase) within the less regular time series.

When the dynamics are following the uncorrelated attractor, the apparent return map for the local dynamics of one of the patches looks like a logistic map with noise. The distribution of densities is very different from that found for an isolated patch, however (Fig. 6). In an isolated logistic map with large r, the population is frequently at its maximum and minimum values. In the uncorrelated attractor, by contrast, the local densities achieve these extreme values only rarely. This is a consequence of transient periodicity: the trajectory spends a lot of time shadowing the out-of-phase two-cycle, which does not attain the lowest population densities.

3.4. Destabilization of the Strictly In-Phase Dynamics

The destabilization of the strictly in-phase chaotic orbit is a statistical phenomenon, as the relative strengths of the contracting and expanding parts of the dynamics shift. Although the long-term trend changes from convergence to divergence, the deviations from that trend are almost identical on both sides of the bifurcation. This is unlike the bifurcations of equilibria and periodic orbits; we suspect that it is a crisis, in which the stable manifolds
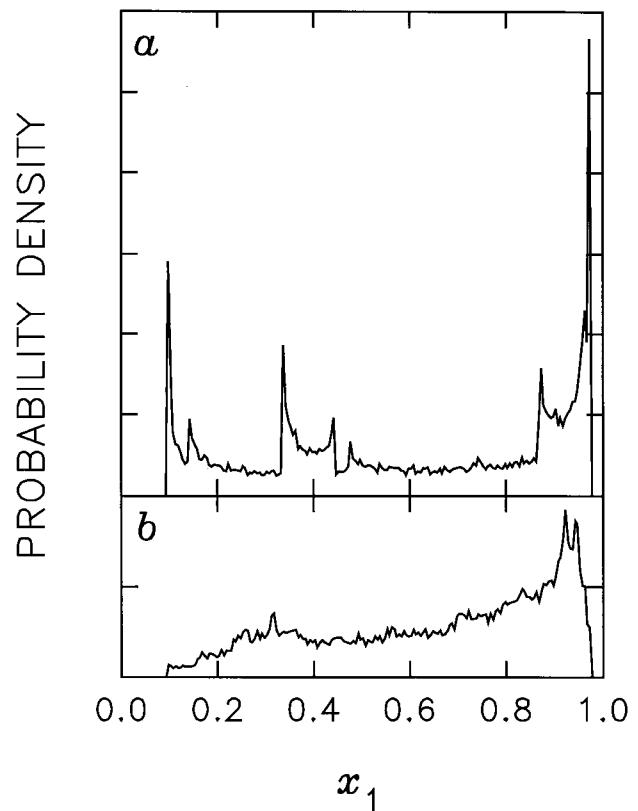
of the out-of-phase orbits come arbitrarily close to the diagonal.

If any out-of-phase dynamics are stable when the strictly in-phase orbit is destabilized, all orbits go to one of the out-of-phase attractors. This is easy to understand, as the approximately in-phase attractor cannot coexist with a stable strictly out-of-phase cycle (the cycles are on its boundary) and the uncorrelated attractor cannot coexist with any stable approximately out-of-phase orbits (it would have to contain them). Thus the destabilization of the strictly in-phase dynamics represents an unusual situation in which a global bifurcation (crisis) can be identified via linear stability analysis. We conjecture that this will be possible whenever the dynamics in question lie on an invariant manifold with dimension one (or more) less than the dimension of the full state space.

If all of the out-of-phase periodic orbits are still saddles when the chaotic in-phase orbit is destabilized, then the approximately in-phase dynamics become globally attracting. All of the existing out-of-phase saddles lie on the boundary of the approximately in-phase dynamics (Fig. 7);
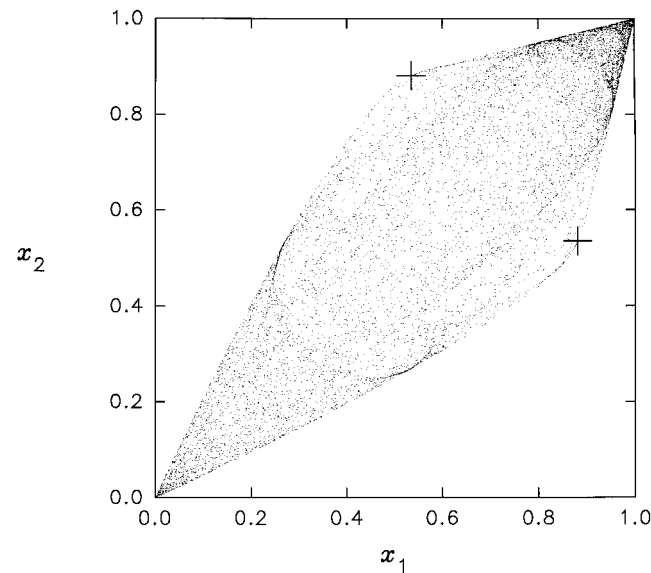
FIG. 7. An approximately in-phase chaotic attractor. $r = 4$, $D = 0.1992$. The saddle strictly out-of-phase two-cycle is indicated by +.

the lines of dense points follow the stable manifolds of these saddles. This attractor exhibits intermittency (episodes of nearly periodic dynamics; Pomeau and Manneville, 1980) as the trajectory nears these orbits.

If all of the out-of-phase orbits have been destabilized by crises when the in-phase orbit is destabilized, then the resulting uncorrelated dynamics are globally attracting. This attractor looks qualitatively similar to the approximately in-phase attractor, but its internal topology is quite different.

3.5. Spatial Structure: Synthesis

The preceding sections contain a lot of information, and they may seem overwhelming. However, the various types of attractor fit together in a relatively simple way, which we summarize here.

Consider a transect through parameter space in which r is increasing, or D is decreasing, or both; as long as the transect ends up in the upper left of parameter space the picture is qualitatively similar. An example (with increasing r) is shown in Fig. 8. Initially the strictly in-phase dynamics are globally attracting. Out-of-phase periodic orbits arise via spatial period-doublings of the
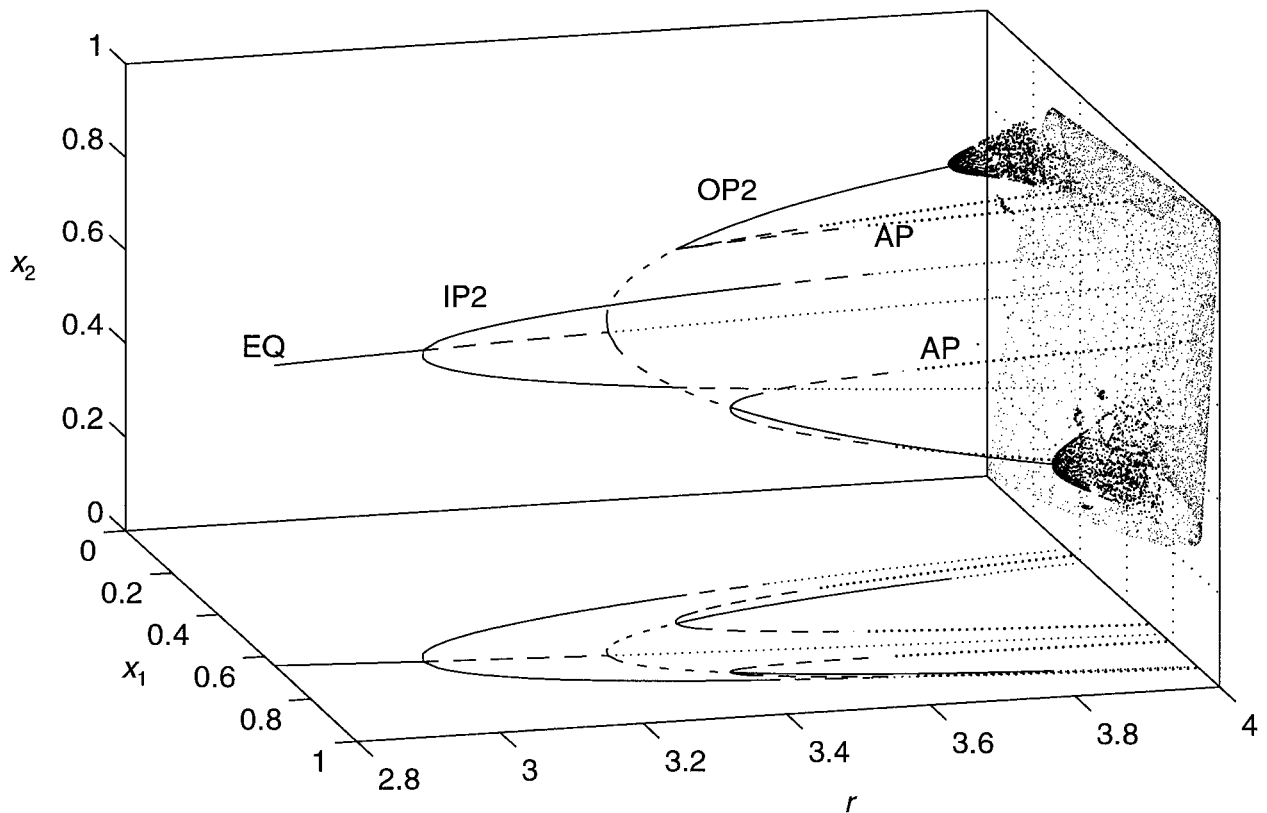

FIG. 8. Bifurcation diagram of the coupled logistic model exhibiting spatial structure; $D = 0.1$. Solid lines are stable orbits, dashed lines are saddles, and dotted lines are unstable orbits. The uncorrelated attractor is shown on the back plane of the diagram.

in-phase orbits. These orbits are initially saddles, become stable via pitchfork bifurcations, and are destabilized again by Naimark bifurcations. The latter produce out-of-phase tori, which in turn become chaotic. The out-of-phase chaotic attractors are destabilized by crises, leading to uncorrelated dynamics.

Somewhere along the way the strictly in-phase dynamics have lost local stability. This always occurs after the out-of-phase two-cycle has appeared; often some of the out-of-phase orbits are already stable, such that there are multiple attractors. If the out-of-phase orbits are still unstable when the diagonal is destabilized then the approximately in-phase dynamics become globally attracting; otherwise the only attractors are out-of-phase.

The uncorrelated attractor contains topological elements from both the in-phase and out-of-phase dynamics, and indeed it is possible to identify transient episodes of both types of behavior in the time series. We have not done any comprehensive analysis of the effects of noise in this study, but we have noted that adding noise when there are coexisting in-phase and out-of-phase attractors can produce patterns similar to uncorrelated dynamics, as the noise switches the system back and forth between the two attractors.

The local stability of the strictly in-phase dynamics depends on an interaction between dispersal and the complexity of the local dynamics. When are the strictly in-phase dynamics globally stable? Gyllenberg *et al.* (1993) conjecture that the global stability criterion is Eq. (III.2), the spatial period-doubling of the equilibrium. With larger dispersal rates than this, there are no equilibria or periodic orbits except on the diagonal, so the diagonal is almost certainly globally attracting. What about smaller dispersal rates? The strictly in-phase dynamics are the only attractor present in most of the region between Eq. (III.2) and the closer of Eqs. (III.3) and (III.4) (where the out-of-phase two-cycle is a saddle and the strictly in-phase dynamics are locally stable; Fig. 1). The only exception we have found is for large r, where the out-of-phase four-cycle is stable at larger D than is the out-of-phase two-cycle. This is not global attraction in the strictest sense, for the out-of-phase saddles are not in the basin of attraction of the strictly in-phase attractor. Almost all initial values are attracted to the diagonal, however, so it is global attraction in a practical sense.

4. ENVIRONMENTAL HETEROGENEITY ALONE

We turn now to environmental heterogeneity, which is the exact opposite of spatial structure: the dispersal rate is high ($D > 0.25$) and the patches differ in quality ($r_1 \neq r_2$). In contrast to the variety of spatial patterns that can arise under spatial structure, all of the attractors under environmental heterogeneity are in-phase. In this section we explore some of the subtleties that underly this simplicity. We require several new quantities: the mean population density, $\bar{x} = (x_1 + x_2)/2$; the mean growth rate parameter, $\bar{r} = (r_1 + r_2)/2$; and the difference between the growth rates in the two patches, $\triangle r = |r_1 - r_2|$.

4.1. Dynamics of Mean Population Density

When there is complete mixing each generation ($D = 0.5$), then the global attractor is strictly in-phase, with dynamics governed by the logistic map with the mean value of r (Proposition 9). When $D < 0.5$, there is no exact solution for the dynamics of $\bar{x}$. Numerical simulations indicate that the in-phase attractor remains globally stable, but it no longer lies on the diagonal (which is not even an invariant manifold). The relationship between x_1 and x_2, however, is very nearly linear. As D decreases, the attractor thickens, making the transverse structure more apparent (Fig. 9a). Furthermore, the slope of the attractor (in the x_1–x_2 plane) deviates progressively more from one.

Nevertheless, Proposition 9(ii) is still a very good approximation even when D is substantially less than 0.5 (Fig. 9). This approximation starts to break down for smaller values of $\bar{r}$, however. In Fig. 10 we show the major bifurcations for several values of D. The boundaries of the period-3 window are essentially unaffected by the value of D: they occur near where one would expect for a single logistic map with $r = \bar{r}$. Similarly, bifurcations in the parameter region of one-piece chaos change little with increasing D. However, when $D < 0.5$ the bifurcations of the period-doubling sequence, as well as the final band-merging creating the one-piece attractor, occur at a lower value of $\bar{r}$ than would be expected by the simple approximation. This effect increases with increasing $\triangle r$ and decreasing D. At the extreme, when $D = 0.25$ and $\triangle r = 4$, the equilibrium period-doubles at $\bar{r} = 2$.

Even when the attractor is thickened in the middle, the upper and lower ends converge into points; we can define the "slope" of the attractor as the slope between those lower and upper points (this is just the ratio of the ranges of x_1 and x_2). This slope depends in a simple way on D, $\bar{r}$, and $\triangle r$. We investigated this relationship with numerical simulations. We chose values of D from 0.25 to 0.5 in steps of 0.01, $\bar{r}$ from 3.7 to 4.0 in steps of 0.01, and $\triangle r$ from 0 to 0.64 in steps of 0.01. For the smaller values of $\bar{r}$ we used a smaller range of $\triangle r$ to ensure that the attractor was a single piece. For each combination of parameters, we initialized the system at $(x_1, x_2) = (0.1, 0.2)$,
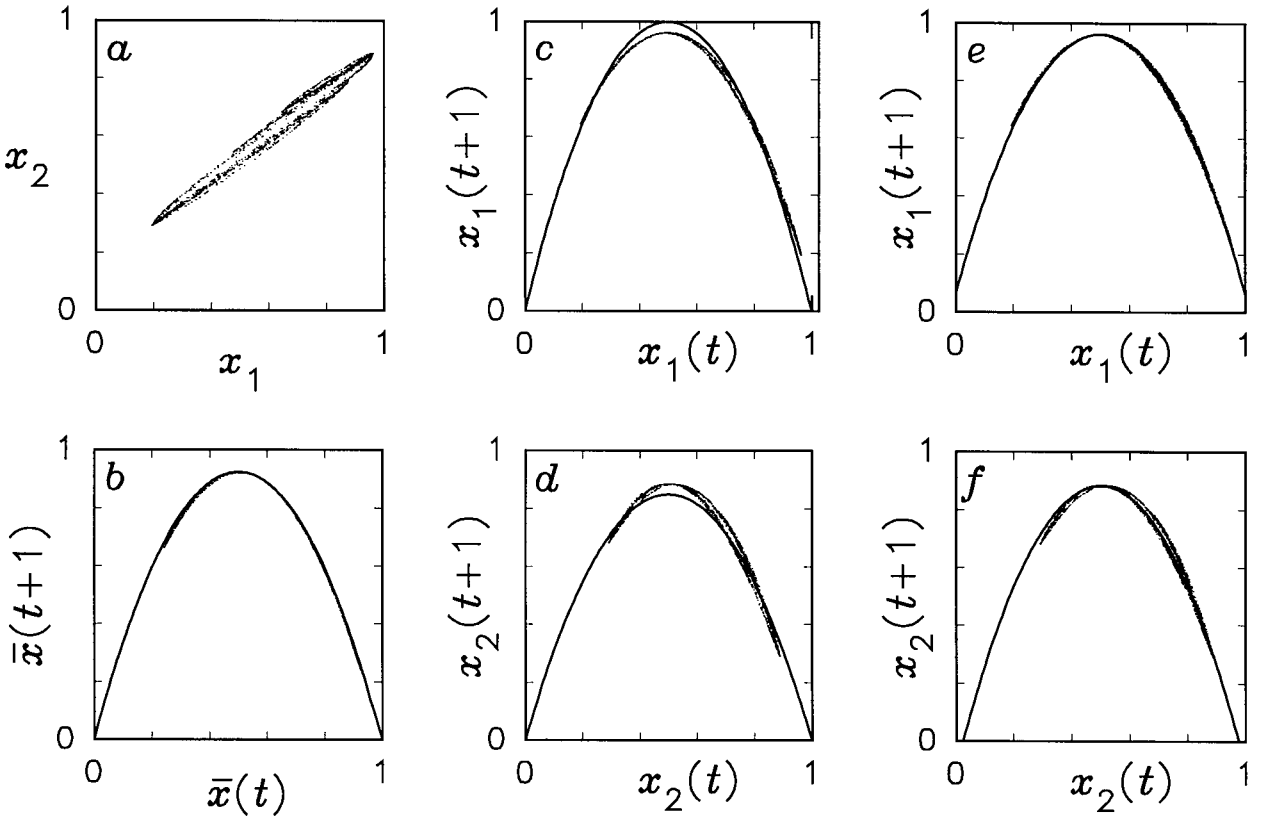
FIG. 9. Approximately in-phase dynamics under environmental heterogeneity. $\bar{r} = 3.7$; $\triangle r = 0.6$; $D = 0.25$. (a) Phase portrait of the attractor. (b) Return map of the mean population size, $\bar{x}$. The points are generated by the map; the curve is $\bar{x}' = 3.7\bar{x}(1 - \bar{x})$. (c) Return map for x_1. (d) Return map for x_2. The curves are the logistic map with local value of r: $r_1 = 4$, $r_2 = 3.4$. (e) and (f) Same as (c) and (d), except that fitted curves are logistic map with constant immigration/emigration added: $x_1' = 0.066 + 3.58x_1(1 - x_1)$, $x_2' = -0.091 + 3.90x_2(1 - x_2)$.

allowed the system 1000 iterates to converge to the attractor, and recorded the dynamics for a further 10,000 iterates.

We defined δ to be the absolute value of the deviation of the slope of the attractor from one. Casual inspection of the data suggested that δ varied linearly with $\bar{r}$ and quadratically with $\triangle r$ and $(1 - 2D)$. Since $\delta = 0$ whenever $\triangle r = 0$ or $(1 - 2D) = 0$, we used multiple linear regression to fit

$$\delta = \triangle r(1 - 2D)[\alpha_1 + \beta_1\bar{r} + \gamma_1 \triangle r$$
$$+ (\alpha_2 + \beta_2\bar{r} + \gamma_2 \triangle r)(1 - 2D)] \qquad (3)$$

(Table 4). The fit is extremely close, suggesting that some simple mechanism underlies the phenomenon, but we have not been able to come to any such understanding.

The effects of the parameters on the slope are consistent throughout the range of values covered by this fit: $\partial\delta/\partial\triangle r$ and $\partial\delta/\partial(1 - 2D)$ are always positive and $\partial\delta/\partial\bar{r}$ is always negative. This is in accord with Fig. 10: the

dynamics become less like those in a homogeneous environment as $\triangle r$ is increased and $\bar{r}$ and D are decreased.

4.2. Local Dynamics

Hidden beneath the relative simplicity of the mean population dynamics are fairly substantial deformations of the underlying local dynamics (Fig. 9). The return maps for the local population size are more steeply humped than any logistic map, and the best fit logistic maps substantially underestimate the differences between the populations. In fact, the local dynamics can be closely approximated by a logistic map with a constant immigration term added:

$$x_1' \approx a_1 + b_1x_1(1 - x_1)$$
$$x_2' \approx a_2 + b_2x_2(1 - x_2) \qquad (4)$$

This again misidentifies the local population growth rate; and although the immigration term would indicate that
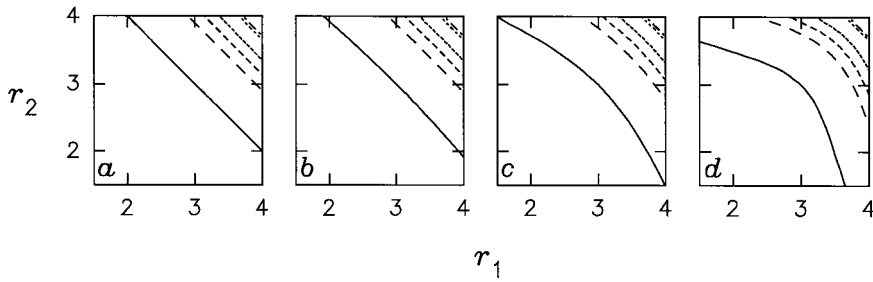
FIG. 10. Bifurcations of the approximately in-phase attractor for environmental heterogeneity. The bifurcations are (in order from the lower left of each panel): period-doubling of the equilibrium; period-doubling of the two-cycle; accumulation of the period-doubling sequence; final band-merging to create a one-piece chaotic attractor; and the lower and upper bounds of the period-three window. (a) $D = 0.5$. (b) $D = 0.45$. (c) $D = 0.35$. (d) $D = 0.25$.

dispersal is important, it misidentifies the true spatial structure.

We examined the effects of parameter variation on model misidentification. We varied the parameters of the coupled logistic model in the same way as described above for the slope of the attractor. For each set of parameter values, we iterated the model for 10,000 iterates and then fit Eq. (4) to the time series. We then fit our estimates of a_1, a_2, $b_1 - \bar{r}$, and $b_2 - \bar{r}$ to Eq. (3) (Table 4). The terms not involving $(\triangle r)^2$ are opposite in sign and roughly equal in magnitude between the two subpopulations. The largest effect, both on the error in the intrinsic growth rate and on the immigration/emigration term, comes from the quadratic relationship with $(1 - 2D)$. The assymetries reflect patterns in the differences between the coefficients of the two populations: $(a_1 - a_2)$ and $(b_1 - b_2)$ seem to depend quadratically on $\bar{r}$ and $\triangle r$, but cubically on $(1 - 2D)$.

4.3. *Environmental Heterogeneity: Summary*

Environmental heterogeneity, with high dispersal rates and differing growth rates in the two patches, only allows one type of attractor: in-phase. The dynamics of mean

TABLE 4

Coefficients of Eq. (3), Describing the Change in Slope of the Attractor (δ), and the Change in the Values of the Coefficients of Eq. (4), with Changes in $\triangle r$, $(1 - 2D)$, and $\bar{r}$

Response	α_1	β_1	γ_1	α_2	β_2	γ_2
δ	0.593	−0.0862	0.0552	3.13	−0.532	−0.402
a_1	2.27	−0.463	−0.157	−5.32	1.27	0.200
$b_1 - \bar{r}$	−6.61	1.31	0.621	13.7	−3.05	−0.834
a_2	−2.37	0.487	−0.0574	5.29	−1.26	−0.184
$b_2 - \bar{r}$	6.19	−1.20	0.378	−10.4	2.14	0.216

population size can be approximated by the logistic map with the mean value of the two growth parameters. This approximation is exact when there is complete mixing each generation ($D = 0.5$), and its accuracy declines with decreasing dispersal and increasing difference between patches.

Within-patch dynamics look deceptively simple: a single patch can be approximated by a logistic map with a constant immigration or emigration term. This structure is qualitatively wrong, and the estimates of the growth rate parameter are also far from the truth. Thus, when there is substantial environmental heterogeneity, it is important to work at the scale of the whole population, or at least recognize that there are spatially mediated interactions that are not apparent from the local dynamics.

5. SPATIAL STRUCTURE WITH ENVIRONMENTAL HETEROGENEITY

In this section we examine the combination of spatial structure and environmental heterogeneity. To do so, we retain $r_1 \neq r_2$, but allow D to be small. Gyllenberg *et al.* (1993) found the regions of stability for the fixed points and both in-phase and out-of-phase two cycles; see their Figs. 5–7.

5.1. *In-Phase Dynamics*

When $r_1 \neq r_2$, the in-phase dynamics no longer occur on the diagonal, but an in-phase attractor may still exist. In fact, for very small $\triangle r$, the in-phase attractor lies very close to the diagonal. In this section we first study the fixed-point and periodic attractors that exist for very small $\triangle r$, and then consider how these results change for larger $\triangle r$. Finally we examine the transition to chaos.

5.1.1. *Analytic approximations.* When $\triangle r$ is very small, there can be attractors homologous to the strictly in-phase attractors that exist when $\triangle r = 0$; they lie very close to the diagonal. When chaotic, they are nearly one-dimensional. Thus we can get an approximate understanding of the in-phase dynamics by studying the eigenstructure of the Jacobian along the diagonal.

The eigenvalues are given by

$$\lambda_i(x)$$
$$= \left[\bar{r}(1-D) \pm \sqrt{\bar{r}^2 D^2 + (\triangle r)^2 (1-2D)/4} \right](1-2x).$$
$$(5)$$

$|\lambda_1(x)|$ increases, and $|\lambda_2(x)|$ decreases, with increasing $\triangle r$. The eigenvectors do not, of course, line up exactly parallel and perpendicular to the diagonal, but the deviations are small if $\triangle r$ is small enough and D is not too small. The directions are still independent of x and they are always perpendicular to each other, but they rotate slowly as the parameters are varied.

If we make the approximation that the "on-diagonal" dynamics are one-dimensional, then we can reconstruct those dynamics by integrating $\lambda_1(x)$. The result is

$$x' = \left[\bar{r}(1-D) + \sqrt{\bar{r}^2 D^2 + (\triangle r)^2 (1-2D)/4} \right] x(1-x).$$
$$(6)$$

The term in the square brackets can be thought of as the "effective r," i.e., this term takes the place of r in the discrete logistic map. It is greater than $\bar{r}$ by the $(\triangle r)^2 (1-2D)/4$ term. This means that, for a given $\bar{r}$, the "effective r" increases with increasing $\triangle r$. Moreover, this effect is magnified by decreasing D. In other words, the effect of increasing r in the one-dimensional case can be mimicked here by increasing the variation among patches and decreasing the dispersal rate between them. This is exactly the effect we already showed for pure environmental heterogeneity.

The second eigenvalue, however, decreases with increasing $\triangle r$. This means that the in-phase dynamics will be locally attracting at a lower value of D than when $\triangle r = 0$. Thus, environmental heterogeneity makes in-phase dynamics more likely to be attracting, but it also makes those dynamics more complex.

5.1.2. *Fixed points and cycles.* As the value of one of the r's is increased slightly while the other is held constant, the fixed point moves slightly off the diagonal: the equilibrium value is higher in the patch with the larger r. Similarly, the points visited on periodic attractors deviate slightly from those visited in the equal r's case; the patch with the higher r has larger-amplitude oscillations.

As suggested by Eq. (5), the eigenvalues deviate slightly from those that occur when $r_1 = r_2$: one of the new eigenvalues is slightly larger, and the other slightly smaller, than in the symmetric case. Period-doublings occur at smaller values of $\bar{r}$ than in a homogeneous environment. For example, when $\triangle r = 0.1$ and $D = 0.1$, the initial period-doubling occurs at $\bar{r} \approx 2.992$, rather than $\bar{r} = 3$.

The eigenvectors of the in-phase periodic orbits rotate as $\bar{r}$ is increased. This is an intriguing phenomenon, but, despite extensive numerical investigations, we have not been able to determine either the cause of the rotation or the effects on the chaotic in-phase attractors that are present at larger $\bar{r}$.

5.1.3. *Onset of chaos.* Past the accumulation point of the period-doubling cascade, the chaotic bands are nearly one-dimensional and parallel to one another, but they are not aligned (Fig. 11a). As $\bar{r}$ is increased, these bands grow longer; but they overlap, rather than meeting. How then does band-merging occur? At some point there is a crisis: the trajectory leaves the bands and follows another path for a while, eventually settling on the adjacent band (Fig. 11b). We do not know what causes this crisis, but we speculate that unstable out-of-phase periodic orbits are involved. As $\bar{r}$ is increased further, the transition sequence between the two bands becomes ever more frequently traveled, resulting in a hollow parallelogram; eventually the center fills in (Figs. 11c and 11d). This new band of period 2^{n-1} is thickened, with a high density of
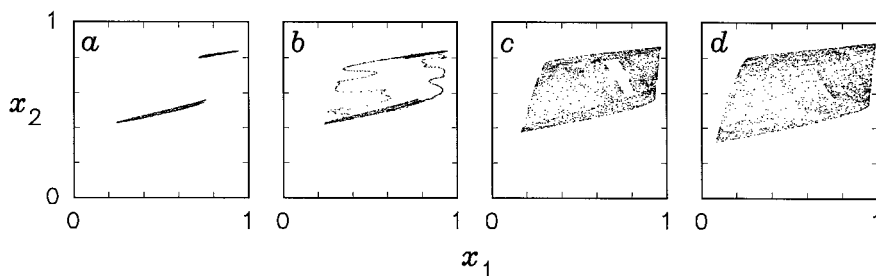

FIG. 11. In-phase dynamics with spatial structure and environmental heterogeneity, showing the final band-merging of the approximately in-phase attractor. $\triangle r = 0.5$ and $D = 0.1$ throughout. (a) $\bar{r} = 3.55$. (b) $\bar{r} = 3.56$. (c) $\bar{r} = 3.65$. (d) $\bar{r} = 3.75$.

points in the regions corresponding to the former bands. This process goes on at each band-merging, so that the final merging to a one-piece chaotic attractor results in a large, diamond shaped attractor rather similar to the approximately in-phase attractor of the equal r's case, except that here there are clusters of points corresponding to higher-order bands (Fig. 12a). If D is small enough, the in-phase dynamics may be destabilized (through a boundary crisis) before it reaches the last band-merging; in that case the out-of-phase dynamics become globally attracting (Fig. 12b).

5.2. Out-of-Phase Dynamics

The dominant collection of out-of-phase dynamics is organized around the two-cycle. We found the bifurcations of these orbits and attractors numerically (Fig. 13). We were not able to make rigorous analytic determinations of the bifurcation types, but using the nature of the stability changes and analogies to Section 3, we could make some high-probability guesses. The out-of-phase two-cycle arises through a period-doubling bifurcation off of the equilibrium. It is initially a saddle; it is stabilized by a pitchfork bifurcation. If $\triangle r$ is large enough, however, then the saddle two-cycle period-doubles along its stable direction before it reaches the pitchfork bifurcation; the resulting four-cycle is a saddle, which in turn either period-doubles or is stabilized by a pitchfork bifurcation. At extreme values of $\triangle r$, the saddle out-of-phase

orbits can period-double all the way to chaos without being stabilized. It is unclear what role the pitchfork bifurcation is playing here. The dynamics are reminiscent of a crisis, but it is possible that a critical periodic orbit on the boundary of the chaotic orbit changes stability from an unstable node to a saddle.

Within the stability region, there are two qualitative sets of bifurcations. When $\triangle r$ is small, then we see the familiar Naimark bifurcation to a two-torus, which goes through a complex set of phase lockings to chaos. When $\triangle r$ is large then, the out-of-phase two-cycle goes through a period-doubling route to chaos. The multi-piece chaotic attractors that result from this are Hénon-like (many folded bands, in contrast to space-filling hyperchaos); at some point in the band-merging sequence (usually from eight to four) there is a crisis rather than a true band-merging, and the hyperchaotic attractor is formed. The four-cycle also arises via a tangent bifurcation from the two-torus: this shows that the whole period-doubling sequence can be considered part of the $2 \times \frac{1}{2}$ locking region of the torus. Indeed, the relationship of the four-cycle to the two-torus suggests that there are actually two pairs of four-cycles. This would indicate that the "period-doubling" is actually a Naimark bifurcation directly into a locking region.

There is a region where the period doubling stops at 8, and the 8-cycle undergoes a Naimark bifurcation. The resulting 8-torus is only present in a very small region of parameter space, however.
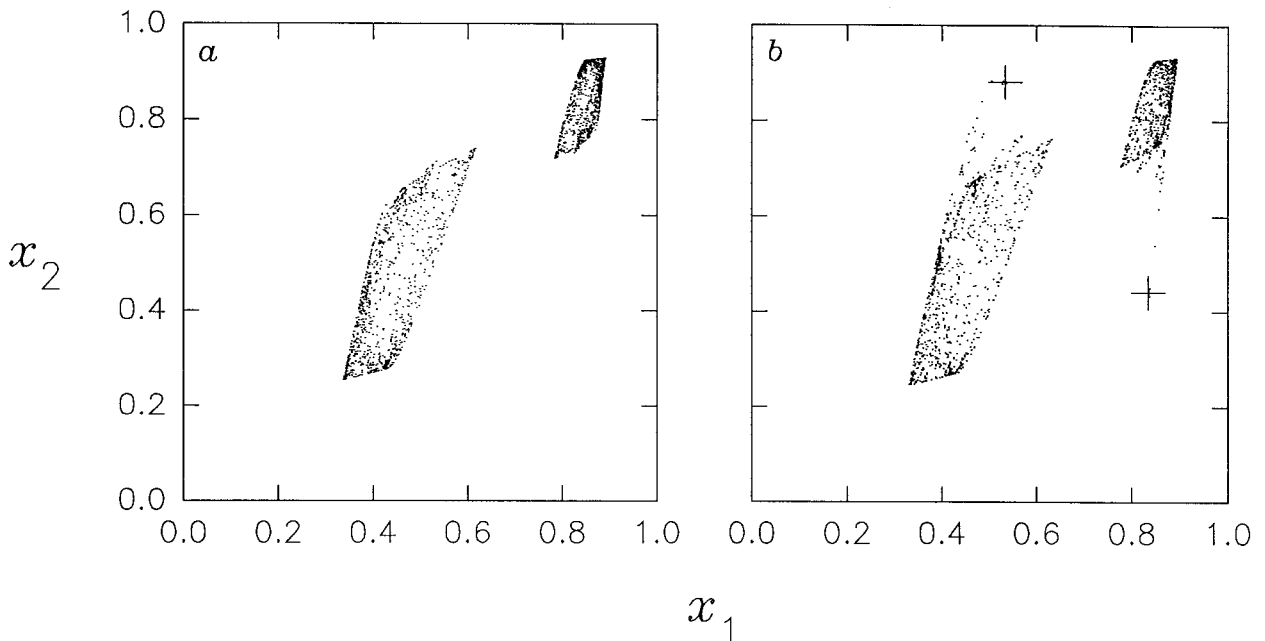

FIG. 12. Approximately in-phase dynamics for (a) $\bar{r} = 3.637734$ and (b) $\bar{r} = 3.649391$. In both cases, $D = 0.1$, $\triangle r = 0.1$. In (b), the in-phase trajectory is a long transient: it eventually converges to the out-of-phase two-cycle (marked $+$).

The out-of-phase orbits lose their stability on the upper right through an interior crisis: the structures of the chaotic out-of-phase orbits can be seen in the transient periodicity of the ensuing uncorrelated attractor. If $\triangle r$ is extremely large, then none of the out-of-phase orbits are ever stable, and there is a direct transition from in-phase to uncorrelated dynamics.

As D is increased, there is very little change in the qualitative nature of the bifurcation structure. The only major change is one we have already seen: when D is small, the two-torus goes to chaos by way of the four-cycle, whereas for larger D the transition is much more confused as many locking regions are encountered. The total size of the parameter region for which the out-of-phase dynamics are stable decreases somewhat with increasing D, and the whole structure moves in the direction of increasing r. These two quantitative results were noted by Gyllenberg *et al.* (1993), who examined the stability of the out-of-phase two-cycle. The other major effect is that the area of parameter space containing quasiperiodic motion on the two-torus increases with increasing D.

The other out-of-phase periodic orbits generate identical bifurcation structures, albeit in miniature. The only one commonly encountered is that of the four-cycle, which largely overlaps the lower left portion of the two-cycle's stability region. All of the higher-order orbits lose their stability at relatively low values of $\triangle r$.

5.3. Uncorrelated Dynamics

When $\triangle r$ is small, the uncorrelated attractor is similar to the one found in the symmetric model: roughly diagonal, hyperchaotic, with strong transient periodicity from the out-of-phase period-two orbits. It is found in the narrow region between the crisis that destabilizes the out-of-phase orbit and the $r = 4$ axes (at the top and right of Fig. 13). Its shape is increasingly skewed as $\triangle r$ increases (Fig. 14); this is accompanied by the dropping out of the higher-order out-of-phase orbits.

When $\triangle r$ is so large that the out-of-phase orbits are never stable, a different picture emerges. Recall that in the case of environmental heterogeneity, the "band-merging" of the approximately in-phase attractor is actually a crisis. This continues to be true for $D < 0.25$, but the difference is that the slope of each of the pieces of the "in-phase" attractor is extremely different from one. Thus the crisis produces a nearly rectangular attractor, with the structures of the two-piece attractor forming its upper and lower boundaries (see Fig. 11). This attractor is so thick that calling it "in-phase" becomes problematic; the resulting "slope" (along the diagonal) is also very different from
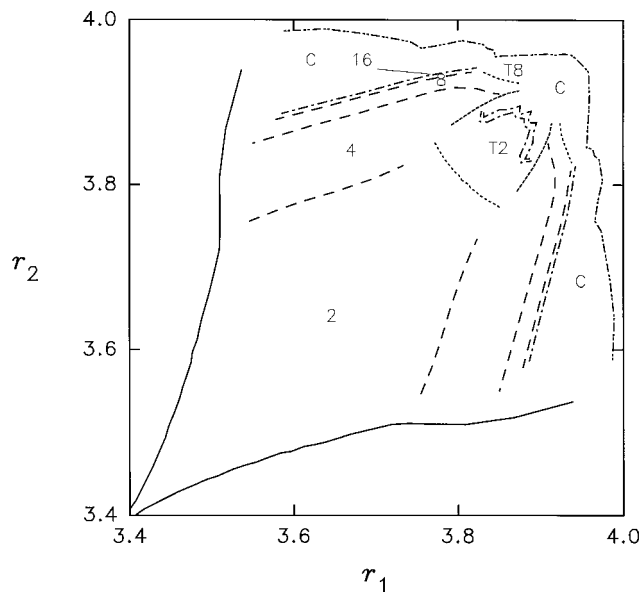

FIG. 13. Bifurcations of the out-of-phase orbits with spatial structure and environmental heterogeneity; $D = 0.1$. Solid lines: pitchfork bifurcations. Long-dashed lines: period-doubling bifurcations. Short-dashed lines: saddle-node bifurcations. Dotted line: Naimark bifurcation. Dash-dotted lines: transition to two-chaos. Dash-double-dotted lines: crisis that destabilizes the out-of-phase attractor. The numbers are the periods of the orbits; "T" denotes torus and "C" denotes chaos.

the slopes of the individual pieces of the two-piece attractor. This attractor also has transient periodicity; but it derives from the in-phase periodic orbits, rather than the out-of-phase ones.

We do not yet fully understand the transition between these two types of uncorrelated attractor. It seems to be smooth, however, with the relative intensity of the transient periodicity gradually shifting from out-of-phase to in-phase. At extreme values of $\triangle r$, and especially for small D, the two types of two-chaos are very similar (essentially parallel structures), and without knowledge of their topological provenance we would have difficulty distinguishing them. There still are many topological mysteries, especially regarding the existence of the out-of-phase periodic orbits, that are largely unresolvable.

5.4. Spatial Structure and Environmental Heterogeneity: Summary

When environmental heterogeneity is added to spatial structure, then all of the qualitative dynamics of spatial structure alone, except the strictly in-phase and strictly out-of-phase dynamics, remain. Environmental heterogeneity does introduce quantitative changes in the dynamics.

When the difference between the patches is small, then the dynamics are qualitatively similar to those produced
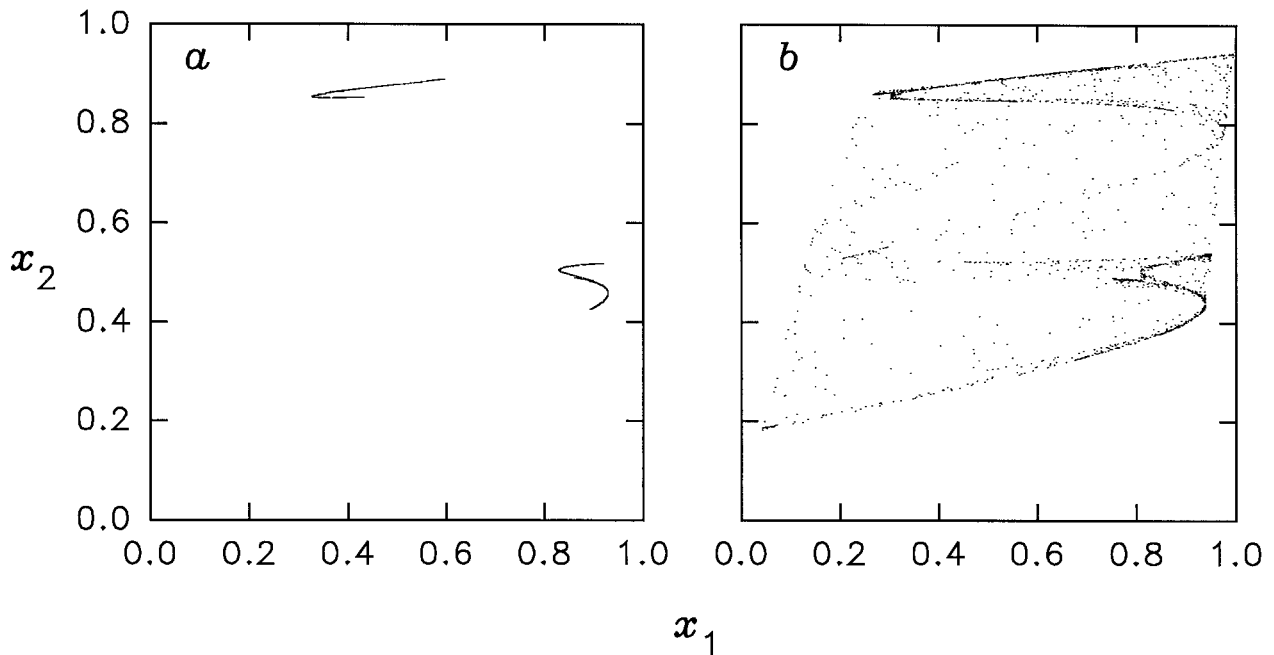
FIG. 14. Transition from out-of-phase to uncorrelated dynamics under spatial structure and environmental heterogeneity. (a) Out-of-phase chaos: $\bar{r} = 3.825$, $\triangle r = 0.25$, $D = 0.1$. (b) Uncorrelated dynamics: $\bar{r} = 3.875$, $\triangle r = 0.25$, $D = 0.1$.

by spatial structure alone. Strictly in-phase dynamics do not exist, but there are tightly correlated approximately in-phase dynamics. These dynamics remain attracting at lower dispersal rates than would be predicted by the mean growth rate, but the temporal dynamics are more complex, just as they are under environmental hetero-geneity alone. The out-of-phase and uncorrelated dynamics are also little changed by mild environmental heterogeneity.

At intermediate levels of environmental heterogeneity, the out-of-phase dynamics change qualitatively. The eigen-values of the out-of-phase two-cycle never become complex, and the two-cycle period-doubles to chaos. Higher order out-of-phase orbits, such as the four-cycle, are never stable unless environmental heterogeneity is small, and even the out-of-phase two-cycle disappears at very large levels of environmental heterogeneity.

6. DISCUSSION

Our primary goal in this paper was to establish a comprehensive baseline upon which to build our further understanding of spatially structured populations. We have developed a fairly complete analysis of the coupled logistic map under the circumstances representing spatial spatial structure (low dispersal) and environmental heterogeneity (unequal patches). We have synthesized

existing analysis and phenomenology, together with a variety of new results, to show how the various patterns generated by this surprisingly complex model fit together. When both aspects of spatial structure are involved the patterns are less clear-cut, but we have provided sketches of the phenomena and how they relate to one another.

We expect that many of the results from this simple model will generalize to more spatially extensive and biologically complex models. As a preliminary assess-ment of this generality we compared our results with those reported for a variety of similar models, mostly from mathematical physics (Appendix B). The stability criterion for the strictly in-phase orbits holds whenever dispersal is density-independent, regardless of the local map or the size of the system. The bifurcation structures of the out-of-phase orbits seem to be generic to diffusively coupled single-hump maps, and many of the qualitative details are retained with non-diffusive coupling. Further-more, analogies of many of the features of the simple model can be found in larger systems. Our results seem to be most sensitive to changes in the dispersal function. Density-dependent dispersal may destabilize equilibria that would be stable in the absence of space (Ruxton, 1996). Asymmetric dispersal rates, which might be caused by prevailing winds or the slope of a hillside, can increase the propensity towards out-of-phase dynamics (Doebeli,

1995). In a one-dimensional array of sites with one-way dispersal, as might be found in a stream, the complexity of the local dynamics increases with increasing distance downstream (Kaneko, 1985).

The coupled logistic map is clearly not a model of real populations. Nevertheless, as a simple metaphor for spatially structured populations, this model has inspired a number of preliminary conceptual generalizations, which we present here. This is not meant as a comprehensive interpretation of all our mathematical results, but rather a selection of certain striking phenomena that have changed the way we think about spatio-temporal population dynamics.

In-phase dynamics represents an absence of spatial pattern. In the coupled logistic map, these dynamics occur if dispersal is large relative to local instabilities; if the within-patch dynamics are stable, then the in-phase dynamics are always at least locally stable. The relationship among the stability of the strictly in-phase orbits, the dominant Lyapunov exponent of the local dynamics, and the strength of the coupling is robust for density-independent dispersal, not only for alternate forms of local dynamics, but also for larger systems. We expect that a similarly simple relationship will hold for any type of density-independent dispersal.

When the patches are identical, the lack of spatial pattern associated with the in-phase dynamics means that spatial structure truly can be neglected in studying the dynamics of the population. Care needs to be taken, however, if the in-phase attractor is not globally stable: a sufficiently large spatially uncorrelated perturbation might knock the population onto an alternate attractor that does display spatial pattern.

Synchronization of patches is also found in the presence of environmental heterogeneity. Indeed, the effects of heterogeneity may be difficult to observe in the field, for there is little change in the nature of the local population dynamics across large changes in habitat quality. However, ignoring the spatial heterogeneity gives only a coarse-grained view of the dynamics, and has little value for predicting the response of the population to habitat change. Heterogeneity could even mislead attempts to understand population dynamics at a smaller spatial scale. Suppose a model were developed to describe the local population dynamics, and the relevant parameters were estimated directly, through measurements of birth and death rates, for example. Even if the model were largely correct, failure to take into account the spatial structure of the population would lead to serious discrepancies between the predicted and observed dynamics. At this stage it is important to recognize that the error lies not in the form of the local model, but in the discounting of spatial effects. This also shows the hazards of parameter estimation through curve fitting, rather than direct measurement. A simple model might fit the local or global dynamics quite well, giving the illusion of understanding; only direct measurements of vital rates would reveal that the fitted parameters are not actually observed anywhere, and that spatial structure underlies the apparent simplicity of the global dynamics.

When there is both spatial structure and environmental heterogeneity, then the "in-phase" dynamics cease to resemble anything we would call spatial synchrony, unless the system is at an equilibrium or two-cycle. The intrinsic dynamics in the two patches are very different, and dispersal is not strong enough to average them. This makes it easier to recognize the environmental heterogeneity, unless the population is at a global equilibrium.

How common are synchronous population fluctuations in nature? The phenomenon is common in cyclic boreal species, such as Norwegian rodents (Myrberget, 1973; Christiansen, 1983), Finnish grouse (Ranta *et al.*, 1995b), and Canadian hares (Smith, 1983). Extensive monitoring projects on British butterflies, moths, and aphids and Finnish vertebrates reveal that synchrony tends to decline with distance (Pollard, 1991; Hanski and Woiwood, 1993; Ranta *et al.*, 1995a; Lindström *et al.*, 1996; Sutcliffe *et al.*, 1996). This has been interpreted both as evidence for limited dispersal (Ranta *et al.*, 1995a; Lindström *et al.*, 1996) and as evidence that temporal environmental variability is spatially correlated (the Moran effect; Hanski and Woiwood, 1993; Sutcliffe *et al.*, 1996). It is not clear how the Moran effect interacts with the actively desynchronizing forces of low to intermediate dispersal.

Out-of-phase dynamics occur only when dispersal is of intermediate strength; the strength required increases with the complexity of the within-patch dynamics. These out-of phase dynamics produce spatial pattern, and they can only occur in the spatial context. They also introduce a problem of scale. As Hastings (1993) points out, the total population size is constant in the out-of-phase two-cycle. Thus a study conducted only at a regional scale would misrepresent the population as having simple, stable dynamics.

One might object that out-of-phase dynamics are an artifact of the two-patch structure of our model. However, there is some empirical evidence for the phenomenon. Studies of mites (Nachman, 1981) and beetles (Nakamura and Ohgushi, 1983) present figures suggesting that strongly linked patches are fluctuating in phase, whereas across weak links the oscillations are systematically out of phase. The required information—moderately long time series collected at the subpopulation level, together with

independent assessments of the relative strength of dispersal among the various patches—have been collected in a number of other systems, but have not been published in sufficiently detailed form to allow us to interpret them.

Models with more than two patches also find spatial pattern. Many of these are host-parasitoid models (Hassell *et al.*, 1991; Comins *et al.*, 1992; Rohani and Miramontes, 1995; Comins and Hassell, 1996), in which the mechanism producing the pattern is likely to be qualitatively different (more like the activation/inhibition of excitable media, often leading to spiral waves). One- or two-dimensional arrays of coupled logistic maps with local dispersal can generate patterns where each subpopulation is out of phase with all of its neighbors (Kaneko, 1987; Kaneko, 1989b). In a one-dimensional array of single-species maps with long range dispersal (dispersal declines with distance), moderate dispersal can lead to spatial waves, in which each subpopulation is fluctuating in a two-cycle, but at a given time there is a sinusoidal pattern in density through space (Ruxton and Doebeli, 1996). This is clearly a long-range analogue to out-of-phase dynamics.

The patterns of local dynamics in the uncorrelated attractor show that even small amounts of dispersal can have large impacts on the local dynamics. A subpopulation of the coupled system is much less likely to have a very low population size than is an equivalent isolated population; this puts it at a lower risk of local extinction. This process, in which spatial structure enhances local persistence, is analogous to the "rescue effect" (Brown and Kodric-Brown, 1977): immigrants from outside the subpopulation prevent the local population size from reaching the extreme lows that would be generated by its intrinsic dynamics.

When one of the *r*'s is less than one, the model becomes a type of source-sink system (Pulliam, 1988): the population in the low-quality patch cannot persist without immigration from the high-quality patch. Source-sink dynamics have important conservation implications: if we eliminate the source population, then the sink populations, deprived of their source of immigrants, will deterministically go extinct (Pulliam, 1988). The coupled logistic model adds a new twist. Imagine that the growth rate in the source population is very high, and that emigration occurs only if there is marginally suitable habitat to go to (or that emigrants, if they find no suitable place to settle, return to their natal patch). As long as the sink patch is present, the dynamics of the source population will be stable. Elimination of the sink habitat, however, will destabilize the source population, and the ensuing large-amplitude oscillations in population size may lead to stochastic extinction. A similar result appears in a two-patch host-parasitoid model (Holt and Hassell, 1993), but that model is confounded by the fact that the sink patch is also a refuge from parasitism.

In a study of ten globally coupled logistic maps with global perturbations, Allen *et al.* (1993) show that values of *r* that lead to chaos in the uncoupled map reduce the probability of global extinction. Extinction risk rises dramatically in the periodic windows. This phenomenon is explained by our Proposition 1. The dispersal rate they use is low enough that the strictly in-phase chaotic dynamics are always locally unstable, so that the subpopulations would become desynchronized, reducing the risk that all would be near zero simultaneously. Indeed, it seems likely that a rescue effect would have been present, with a reduction in the within-patch probability of low population size. Proposition 1 shows, however, that the periodic strictly in-phase orbits are always locally stable, so that there is a good chance that the subpopulations can become synchronized. This synchronization puts the global population at a much higher risk of extinction. However, the average duration of the the asynchronous chaotic transients increases exponentially with the number of patches (Kaneko, 1990), so that this phenomenon will not be observed in large systems.

We have not considered the effects of noise in this analysis. Much of the fine structure, such as the small periodic windows, will disappear when noise is added. We would like to know which of the phenomena we report will persist in the presence of noise, for actual populations are always subject to exogenous perturbations. Our experience, however, is that to understand the effects of noise in nonlinear systems such as the coupled logistic map, we must first have a thorough understanding of the underlying deterministic dynamics. This paper serves the latter role.

We stated at the outset that developing a theory of spatio-temporal population dynamics is a hard problem. Even in the "simple" model discussed here there is much that still escapes our comprehension. While it is important not to get too caught up in fine-scale deterministic details that will never be realized in actual ecological systems, this complexity underscores the value of starting with simple models to establish our understanding of general phenomena in spatio-temporal dynamics.

APPENDIX A: PROPOSITIONS

PROPOSITION 1. *If* $D > \frac{1}{2}(1 - e^{-\Lambda_r})$, *where* Λ_r *is the Lyapunov exponent of the logistic map with parameter r, then the strictly in-phase dynamics are locally stable.*

Proof. This proof consists of a linear stability analysis of the orbit on the diagonal, which we denote $\mathscr{S}_+$. If $\mathscr{S}_+$ is

an equilibrium or cycle then the analysis is conceptually straightforward, although we introduce some tricks to avoid having to calculate the orbit explicitly. If $\mathscr{S}_+$ is chaotic, however, we must address a number of subtleties to make the proof rigorous.

Let $J(x)$ be the Jacobian of Eq. (2) evaluated at $x_1 = x_2 \equiv x$. The eigenvalues of J are

$$\lambda_1(x) = r(1 - 2x),$$
$$\lambda_2(x) = (1 - 2D)\, r(1 - 2x);$$
(A.1)

the associated normalized eigenvectors are $\mathbf{e_1}(x) = (\sqrt{2}, \sqrt{2})$ and $\mathbf{e_2}(x) = (\sqrt{2}, -\sqrt{2})$. The eigenvectors are always parallel and perpendicular, respectively, to the diagonal, and if $0 < D < 1$, $|\lambda_1(x)| > |\lambda_2(x)|$. Also notice that $\lambda_1(x)$ is simply the derivative of the logistic map evaluated at x.

The Lyapunov exponents of $\mathscr{S}_+$ can be estimated by evaluating the Jacobian along each point of an orbit:

$$\Lambda_i(x_0) = \lim_{n \to \infty} \frac{1}{n} \log \| J(x_{n-1})\, J(x_{n-2}) \cdots J(x_0)\, \mathbf{e_i}(x_0) \|$$
(A.2)

(see, for example, Eckmann and Ruelle, 1985). The logistic map does not contain coexisting attractors, so the dependence of Λ on x_0 is critical only if x_0 is on an unstable periodic orbit (or equilibrium); we choose a "typical" value of x_0 that is not one of these. We can take advantage of the fact that the eigenvectors are independent of x to simplify Eq. (A.2): for example,

$$J(x_1)\, J(x_0)\, \mathbf{e_i}(x_0) = J(x_1)\, \lambda_i(x_0)\, \mathbf{e_i}(x_0)$$
$$= \lambda_i(x_0)\, J(x_1)\, \mathbf{e_i}(x_0)$$
$$= \lambda_i(x_0)\, J(x_1)\, \mathbf{e_i}(x_1)$$
$$= \lambda_i(x_1)\, \lambda_i(x_0)\, \mathbf{e_i}(x_0) \quad \text{(A.3)}$$

(we could not do this if the eigenvectors depended on x). This simplification, together with the fact that $\|\mathbf{e_i}(x_0)\| = 1$, gives

$$\Lambda_i(x_0) = \lim_{n \to \infty} \frac{1}{n} \log |\lambda_i(x_{n-1})\, \lambda_i(x_{n-2}) \cdots \lambda_i(x_0)|$$
$$= \lim_{n \to \infty} \frac{1}{n} \sum_{j=0}^{n-1} \log |\lambda_i(x_j)|.$$
(A.4)

Λ_1 is simply the Lyapunov exponent of the logistic map, and $\Lambda_2 = \Lambda_1 + \log(1 - 2D)$.

If $\mathscr{S}_+$ is a periodic orbit, then we are done: the absolute value of the eigenvalues are e^{Λ_1} and e^{Λ_2}, and we apply standard stability criteria. If both eigenvalues are less than one, then the orbit is stable. In particular, if the orbit is a stable periodic orbit of the nonspatial map ($\Lambda_1 < 0$), then $\Lambda_2 < \Lambda_1$ is also less than zero ($\log(1 - 2D)$ is negative), and the orbit is locally stable in the coupled system.

"Linearizing" around a chaotic orbit is somewhat more subtle. We need first to show that there is a neighborhood of $\mathscr{S}_+$ in which trajectories "shadow" the orbit on $\mathscr{S}_+$, linearly approaching or moving away from the diagonal. The stability of $\mathscr{S}_+$ is then determined by whether or not, on average, trajectories in the neighborhood approach the diagonal.

LEMMA 2. *If $r < 4$, then there exists a neighborhood $\mathscr{N}$ of $\mathscr{S}_+$ with width $\delta > 0$ such that the dynamics in the diagonal direction are governed by the logistic map $+ \mathcal{O}(\delta^2)$ and dynamics in the off-diagonal direction are perpendicular to the diagonal.*

Proof. We proceed by assuming the existence of a neighborhood satisfying the lemma, and show that the required δ is greater than zero.

Reparameterize the system to follow the coordinate frame defined by $\mathbf{e_1}(x)$ and $\mathbf{e_2}(x)$:

$$y_1 = \frac{x_1 + x_2}{2},$$
$$y_2 = \sqrt{2}\, \frac{x_2 - x_1}{2}.$$
(A.5)

In this coordinate frame, y_1 is the perpendicular projection of (x_1, x_2) onto the diagonal and $|y_2|$ is the distance from (x_1, x_2) to the diagonal. The dynamics in this new coordinate frame are described by

$$y_1' = ry_1(1 - y_1) - \frac{ry_2^2}{2}$$
$$y_2' = (1 - 2D)\, ry_2(1 - 2y_1).$$
(A.6)

As long as the trajectory is within $\mathscr{N}$, then $y_2 \leqslant \delta$, and the dynamics along the diagonal are governed by $y_1' = ry_1(1 - y_1) - \varepsilon$, where $\varepsilon \leqslant r\, \delta^2/2$. The distance from the diagonal grows or shrinks linearly in y_2 (although the rate and direction are determined by y_1). Thus if δ is small enough we can approximate Eq. (A.6) by

$$y_1' = ry_1(1 - y_1)$$
$$y_2' = (1 - 2D)\, ry_2(1 - 2y_1).$$
(A.7)

"Small enough" means δ is small compared with the logistic equation over the entire range of y_1 explored by the dynamics. When y_1 is small, $y_1' \approx ry_1 - \varepsilon$, so we require $\varepsilon \ll \min_{\mathscr{S}_+} y_1$ where we take $\min_{\mathscr{S}_+} y_1$ to mean "the minimum value of y_1 attained by an orbit on $\mathscr{S}_+$." This minimum depends, of course, on r. Thus we choose our neighborhood $\mathscr{N}$ to be small enough that $0 < \delta < \min_{\mathscr{S}_+} y_1$. This is possible for all $r < 4$, because $\min_{\mathscr{S}_+} y_1 > 0$. If $r = 4$, then y_1 can come arbitrarily close to zero, and so we cannot find a nonzero value of δ to guarantee the linearization. ∎

We now show that there are trajectories starting near (but not on) the diagonal that remain in $\mathscr{N}$ when $\Lambda_2 < 0$.

LEMMA 3.   *If $\Lambda_2(x) < 0$ for an orbit on $\mathscr{S}_+$ starting at x, then there is an $\gamma > 0$ such that the trajectory starting at (x, γ) and governed by Eq. (A.6) remains within $\mathscr{N}$.*

Proof.   At first glance this proposition seems trivial. However, since Λ_2 is a long term average, we need to take care with sequences $\{x_i\}$ such that $|\lambda_2(x \in \{x_i\})| > 1$ for all i. These might represent "escape hatches" where the trajectory can monotonically move away from the diagonal in spite of the long-term average attraction.

First consider the case where the sequence $\{x_i\}$ is finite, with m elements. If $r < 4$, then for any $\mathscr{N}$ we can choose $\gamma \leqslant [(1 - 2D) r\varepsilon \min_{\mathscr{S}_+} y_1]^{1/m}$ so that a trajectory starting on the escape hatch with $y_2 = \gamma$ will end the sequence with $y_2 \leqslant \varepsilon \min_{\mathscr{S}_+} y_1$. Thus we can always find an initial condition that is close to, but not on, the diagonal such that the finite escape hatch $\{x_i\}$ will not cause the trajectory to leave $\mathscr{N}$.

Are there places where the escape hatches are effectively infinite, so that no matter how small the initial value of y_2, the trajectory will monotonically depart from $\mathscr{N}$? Indeed there are. Any trajectory starting on the unstable manifold (in the $\mathbf{e_2}$ direction) of an unstable in-phase periodic orbit will move monotonically away from the diagonal; and since this manifold is invariant, it does not matter how close to the diagonal the initial condition is. Very close to the diagonal, this manifold is simply perpendicular to the diagonal, with the value of y_1 corresponding to the nonstable periodic orbit of the logistic map. However, although there are an infinite number of nonstable periodic orbits present in the chaotic attractor of the logistic map, and they may be dense, they have measure zero. Thus, just as almost all trajectories of the logistic map will never land exactly on a nonstable periodic orbit, almost no trajectories of the coupled logistic map will land on an infinite escape hatch. ∎

Finally, we need to show that y_2 goes to zero for trajectories in $\mathscr{N}$. Comparing Eqs. (A.6) and (A.1), it is clear that $y_2(n) = y_2(0) \prod_{i=1}^{n} \lambda_2(y_1(i))$. If n is large, then $\log y_2(n) \approx \log y_2(0) + n\Lambda_2$. Since $\Lambda_2 < \Lambda_1 < 0$, $\lim_{n \to \infty} \log y_2(n) = -\infty$, and y_2 goes to zero.

This proof does not work for $r = 4$. However, at that point, the conjectured curve for local stability passes through $D = 0.25$, which is also the value at which we have shown that $\mathscr{S}_+$ is globally attracting. ∎

PROPOSITION 4.   *At the parameter values defined by Eq. (III.2) the equilibrium solution on the diagonal undergoes a period-doubling bifurcation in the off-diagonal direction, giving rise to the two-cycle (II.4). This orbit is a saddle, with $\lambda_1 \geqslant 1$ ($\lambda_1 = 1$ at the bifurcation iff $D = 0$) and $\lambda_2 \leqslant 1$ ($\lambda_2 = 1$ only at the bifurcation).*

Proof.   At Eq. (III.2), λ_2 passes through -1; at this point $\lambda_1 = -(1 - 2D)^{-1}$. Thus the equilibrium, which has already undergone one period-doubling to produce the in-phase two-cycle, period-doubles a second time, in a direction perpendicular to the diagonal. It then becomes a repelling node. The eigenvalues of the resulting out-of-phase two-cycle are $\lambda_1 = (1 - 2D)^{-2}$ (which is the square of the eigenvalue of the equilibrium) and $\lambda_2 = 1$. Thus the out-of-phase two-cycle "inherits" the instability in the diagonal direction from the equilibrium.

Although it seems clear what is happening as curve (III.2) is crossed, we need to ensure that there are not any oddities cropping up as a consequence of the two-parameter, two-variable nature of the system. So we need to first determine whether, in a neighborhood in parameter space of a given point on curve (III.2), and a neighborhood in state space of the equilibrium, the problem can be reduced to a one-parameter, one-variable problem.

The simplest choice for a reparameterization of the problem is to take a line normal to the bifurcation curve. This is everywhere defined, as Eq. (III.2) is everywhere differentiable. Thus our new parameter, μ, defines a curve in the original parameter space given by

$$r = h_1(\mu) = 2 + \frac{1}{1 - 2D_0} + \frac{(1 - 2D_0)^2}{2}\mu \quad \text{(A.8)}$$

$$D = h_2(\mu) = D_0 - \mu, \quad \text{(A.9)}$$

where D_0 is the value of D where the bifurcation curve is crossed. μ is zero at the bifurcation; negative values of μ are below the bifurcation curve. This parameterization is defined everywhere on $0 \leqslant D_0 \leqslant 0.25$.

The bifurcation takes place in the direction of the second eigenvector of the equilibrium, which we already

know from the proof of proposition 1 is perpendicular to the diagonal. Furthermore, the error associated with the linearization grows only as y_2^2, so very close to the equilibrium we can just look at the dynamics along the eigenvector, which is in turn the dynamics of y_2. The value of y_1 is fixed at the equilibrium value of $1 - 1/r$.

Letting $x = y_2$, we can reduce the system locally to

$$f(x, \mu) = (1 - 2h_2)(2 - h_1)\, x \qquad (A.10)$$

$$f^{(2)}(x, \mu) = (1 - 2h_2)^2\, (2 - h_1)\, h_1^2 x^3$$
$$+ (1 - 2h_2)^2\, (2 - h_1)^2\, x. \qquad (A.11)$$

It is now straightforward (but tedious) to show, using the formulas in Wiggins (1990, p. 373), that f undergoes a period-doubling bifurcation at $x = 0$, $\mu = 0$. ∎

PROPOSITION 5. *The strictly out-of-phase two-cycle Eq.* (II.4) *changes from a stable node to a stable focus at Eq.* (III.5).

Proof. This transition occurs when the eigenvalues of the strictly out-of-phase two-cycle change from real to complex. The eigenvalues are

$$\lambda = \Big[\, 2 + 2(1 - 5D)(1 - D) - r(r - 2)(1 - 2D)^3$$
$$\pm 2D\, \sqrt{(2 - 3D)^2 - r(r - 2)(1 - 2D)^3}\, \Big]/(1 - 2D)^2,$$
$$(A.12)$$

which become complex when the quantity under the radical passes through zero. It is easy to show that this occurs at Eq. (III.5). Along this curve $\lambda = D^2/(1 - 2D)^2$, which is less than one if $D < 0.25$, so the orbit is stable at the transition. ∎

PROPOSITION 6. *Along the Naimark bifurcation curve defined by Eq.* (III.6), *the absolute value of the rotation number decreases, smoothly and monotonically, from $\frac{1}{2}$ at $D = 0$ to approximately $\frac{11}{25}$ at $r = 4$.*

Proof. The Naimark bifurcation reaches $r = 4$ at $D \approx 0.13925$. Along the Naimark bifurcation, the rotation number ρ can be evaluated directly from the eigenvalues of the periodic orbit. The eigenvalues are complex: $\lambda = \mathrm{Re}[\lambda] \pm i\,\mathrm{Im}[\lambda]$. We can express this in polar coordinate form: $\lambda = \alpha e^{i\theta}$, where $\alpha = \sqrt{\mathrm{Re}[\lambda]^2 + \mathrm{Im}[\lambda]^2}$ and

$$\theta = \begin{cases} \tan^{-1} \dfrac{\mathrm{Im}[\lambda]}{\mathrm{Re}[\lambda]} & \text{if} \quad \mathrm{Re}[\lambda] > 0, \\[2ex] \pi + \tan^{-1} \dfrac{\mathrm{Im}[\lambda]}{-\mathrm{Re}[\lambda]} & \text{if} \quad \mathrm{Re}[\lambda] < 0 \end{cases} \qquad (A.13)$$

(the latter case is to account for the limited range of $\tan^{-1}$; at the Naimark bifurcation the real part of the eigenvalue is negative, so we use the second case). In the linearized system, α gives the rate of radial movement towards or away from the periodic orbit, and θ is the angular movement as the orbit spirals into or away from the periodic point; $\alpha = 1$ at the Naimark bifurcation. Furthermore, the nonhyperbolic fixed point at the origin can be thought of not only as an equilibrium, but also as an invariant loop with radius zero. The rotation number on this loop is simply the fraction of the circle represented by θ:

$$\rho = \frac{\theta}{2\pi}$$
$$= \frac{1}{2\pi} \tan^{-1} \frac{\mathrm{Im}[\lambda]}{-\mathrm{Re}[\lambda]} + \frac{1}{2}$$
$$= \frac{1}{2\pi} \tan^{-1} \frac{\pm 2D\, \sqrt{(1 - 3D)(1 - D)}}{-(1 - 4D + 2D^2)} + \frac{1}{2}. \qquad (A.14)$$

The absolute value of this function declines monotonically and continuously from $1/2$ at $D = 0$ to about 0.43818 at $D = 0.13925$. Equation (III.6) is thus equivalent to the $K = 0$ line of the circle map, and all the rational values of Eq. (A.14) correspond to the tips of the locking regions with rotation number ρ. ∎

PROPOSITION 7. *Let P_i be the ith strictly out-of-phase orbit to arise as r is increased with $D = 0$ (thus P_1 is the two-cycle, P_2 the four-cycle, etc.), and let $r = h_i(D)$ be the curve along which P_i arises via the off-diagonal period-doubling. Then:*

(i) $h_j(D) < h_i(D)$ *for all $j < i$ and $D < 0.25$; and*

(ii) $h_i(0.25) = 4$ *for all i.*

Proof. From the proof of Proposition 1, we know that h_n is defined by the criterion $\Lambda_1(P_n) + \log(1 - 2D) = 0$, where $\Lambda_1(P_n)$ is the Lyapunov exponent of the n-cycle in the logistic map. The second part of the proposition follows directly from the following lemma:

LEMMA 8. *When $r = 4$, all of the periodic orbits of the logistic map have Lyapunov exponent $\log 2$.*

Proof. We proceed by finding a map that is topologically conjugate to the logistic map at $r = 4$ for which we can show the desired result. Recall that two maps f and g are topologically conjugate if there is a diffeomorphism h such that $g \circ h = h \circ f$. Corresponding fixed points and periodic orbits have the same eigenvalues in f and g (Wiggins, 1988). It is also clear that conjugacy is transitive.

It is widely known that $f(x) = rx(1-x)$ is topologically conjugate to $g(y) = 1 - Ay^2$, where $A = [(r-1)^2 - 1]/4$ and $y = h(x) = r(x - 1/2)/A$. In particular, $r = 4$ is equivalent to $A = 2$. Collet and Eckmann (1980) noted that $g(y) = 1 - 2y^2$ is topologically conjugate to $\gamma(z) = 1 - 2|z|$, where $z = \xi(y) = (4/\pi)\sin^{-1}\sqrt{(y+1)/2} - 1$; the proof of this is straightforward.

Thus the logistic map at $r = 4$ is topologically conjugate to γ. The derivative of γ is ± 2 everywhere except at $z = 0$ (the latter need not concern us, for $\gamma^{(2)}(0) = -1$, which is a fixed point, so $z = 0$ is not on a periodic orbit). Thus all the period-n orbits of γ, and hence of f, have eigenvalue $\pm 2^n$. The Lyapunov exponent of the period-n orbit is $\Lambda_1(P_n) = \frac{1}{n}\sum_{i=1}^{n}\log 2 = \log 2$. ∎

The first part of the proposition follows from the observation (for which we have no formal proof, but which is clear numerically) that, beyond the superstable point (where $\Lambda_1(P_n) = -\infty$), the Lyapunov exponents of all of the periodic orbits increase monotonically with r, and have negative second derivative. Given that all of these curves intersect at $r = 4$, they cannot cross at any $r < 4$. ∎

PROPOSITION 9. *If $D = 0.5$, then*:

(i) *the diagonal is always attracting*; *and*

(ii) *the mean population density is governed by* $\bar{x}' = r\bar{x}(1 - \bar{x})$.

Proof. Since $(1 - D) = D = 0.5$, the governing equations are

$$x'_1 = 0.5r_1 x_1(1 - x_1) + 0.5r_2 x_2(1 - x_2)$$
$$x'_2 = 0.5r_2 x_2(1 - x_2) + 0.5r_1 x_1(1 - x_1). \qquad \text{(A.15)}$$

Thus from any initial condition $x'_1 = x'_2$, and $x_1 = x_2$ thereafter.

Since $x_1 = x_2$, the mean density $\bar{x} = x_1 = x_2$. It is governed by

$$\bar{x}' = x'_1 = x'_2$$
$$= \frac{r_1 + r_2}{2}\bar{x}(1 - \bar{x})$$
$$= \bar{r}\bar{x}(1 - \bar{x}). \qquad \text{(A.16)}$$

APPENDIX B: COMPARISONS WITH RELATED MODELS

We are searching for results that are generally applicable when density dependence interacts with spatial structure.

This requires, at the very least, that the results be mathematically robust to substantive structural changes in the model. In a subsequent study we will systematically vary the local dynamics, the dispersal function, and the size of the system. Here we develop a preliminary assessment of the mathematical robustness of our model by comparing it with published analyses of related models (many without direct biological interpretation). We discuss, in turn, pairs of logistic maps with alternative coupling functions, alternative local maps with diffusive coupling, and models of many logistic maps with diffusive coupling.

A common coupling form in the physics literature is $x'_i = f(x_i) + D(x_j - x_i)$ (Kaneko, 1983; Hogg and Huberman, 1984; Waller and Kapral, 1984; Daido, 1984a,b; Sakaguchi and Tomita, 1987; Wang *et al.*, 1989; Wang and Lowenstein, 1990; Kook *et al.*, 1991). The qualitative phenomenology of this model is very similar to the one we have been examining. Strictly in-phase orbits period-double in both the on-diagonal and off-diagonal directions, the latter producing strictly out-of-phase orbits. The out-of-phase orbits lose stability through Naimark bifurcations; and the transition to hyperchaos through a torus and the destabilization of the approximately out-of-phase chaotic attractors also follows the same qualitative pattern as we have shown. However, the quantitative details are quite different. The spatial period-doubling bifurcations occur at lower values of r than do the non-spatial ones. The stability region of the equilibrium shrinks with increasing coupling (Hogg and Huberman, 1984), showing that coupling need not be inherently "stabilizing." The strictly out-of-phase orbits are stable when they appear, whereas the strictly in-phase orbits are saddles at the period-doubling, gaining stability through a separate pitchfork bifurcation (Sakaguchi and Tomita, 1987; this is the inverse of the results for the system we have studied); unlike our model, there is not a continuous sequence of stable strictly in-phase orbits through the period-doubling cascade. The uncorrelated attractor looks very different from the ones we have studied (Sakaguchi and Tomita, 1987, Figs. 7 and 8).

Another commonly studied form of coupling is $x'_i = f(x_i) + Dx_j$ (Frøyland, 1983; Van Buskirk and Jeffries, 1985; Ferretti and Rahman, 1987a, b, 1988). This also shares many of the qualitative features of our model, including Naimark bifurcations of the out-of-phase orbits, but there begin to be substantial deviations as well. There are large Hénon-like attractors; in our model they only appear as elements of a multi-part chaotic attractor. The onset of period-doublings and chaos occurs at substantially reduced values of r, even for moderate coupling strengths.

A third coupling form is $x'_i = f(x_i)(Dx_j + \varepsilon)$ with $D = 3$ and $\varepsilon = 1$ (López-Ruiz and Pérez-García, 1991, 1992).

The equilibrium period-doubles to an out-of-phase two-cycle, which goes through a Naimark bifurcation and through a torus to chaos; but the chaotic attractor is extremely different from any of the ones we have studied (it does, however, show some similarity to attractors pictured in Kaneko, 1983). The transition from the invariant loops to chaos seems to be very different from the ones we have studied. Moreover, the bifurcations of the equilibrium and the two-cycle occur at very low values of r, all less than one.

There are a few models that use density-independent dispersal, but different models for the local dynamics. Coupled "sigmoidal maps," $f(x) = ax/(1 + x^n)$, display the familiar sequence of uncorrelated chaos, approximately out-of-phase chaos and torus, strictly out-of-phase two-cycle, and strictly in-phase chaos as coupling strength decreases (Doebeli, 1995). The out-of-phase chaotic attractor is nearly indistinguishable from the attractors we have seen (Losson and Mackey, 1994). A similar bifurcation structure was found in a two-patch age-structured model (Hastings, 1992). Losson and Mackey (1994) also couple two tent maps (similar to $\gamma(z)$ in Lemma 8). They show the presence of the four attracting four-cycles (strictly in-phase, strictly out-of-phase, and the anti-phase pair). They obtain the familiar criterion for the local stability of the strictly in-phase orbits, and analytic expressions for transitions such as the crisis from the out-of-phase chaotic attractor to the uncorrelated attractor; the formulas are complicated and not very informative, however. Yamada and Fujisaka (1983) coupled two modified Brusselator models (continuous-time models used to simulate the Belousov–Zaboutinsky chemical reaction). They extracted a mapping by taking a Poincaré section of each oscillator. The result was the familiar collection of attractors: strictly out-of-phase two- and four-cycles, out-of-phase quasiperiodic and chaotic attractors, strictly in-phase attractors, and uncorrelated attractors.

There have been many studies of large arrays of coupled logistic maps (for a review see Kaneko, 1993). Each oscillator can be coupled to all the other oscillators (global coupling) or to its nearest two (one-dimensional space) or four (two-dimensional space) neighbors. As one might imagine, the phenomenology becomes much richer (and harder to describe). There are a few comparisons that can be made with our work, however. The local stability condition for the strictly in-phase orbits in globally coupled maps is identical to our Proposition 1 (Kaneko, 1989a); but the basin of attraction of the strictly in-phase orbits decreases very rapidly with the number of oscillators (Kaneko, 1993). In "fully developed spatio-temporal chaos" there are no periodic windows (Kaneko,

1990). This seems to correspond with observations of our system when the attractors are of the hyperchaotic type. Virtually all of our chaotic attractors that do show periodic windows look similar to attractors of the Hénon map, in that they exhibit folded one-dimensional manifold structure, corresponding to a single positive Lyapunov exponent.

There are a number of attracting states of the larger systems that might be thought of as analogous to our system of two oscillators. With nearest-neighbor coupling, a commonly encountered attractor is temporally periodic with a "zigzag" (one-dimensional) or "checkerboard" (two-dimensional) spatial pattern. In these cases each site is strictly out-of-phase with all of its neighbors, and the dynamics can just as well be described by our model with strictly out-of-phase dynamics. However, our model cannot predict how this spatial symmetry will be broken, nor what will occur when the dynamics are temporally chaotic. In globally coupled maps there is a remarkable region of parameter space where the oscillators cluster into a small number of groups, with the members of each cluster all following the same trajectory (Kaneko, 1989a). If the system settles down to two clusters, then the subsequent dynamics can be described by a two-oscillator system with appropriate weighting of the coupling terms to account for the different size of the clusters. At first glance it seems like a way to model patches with different carrying capacities, but the effect is more subtle than simply inserting K's into our model. It is as if the smaller patch, in addition to producing fewer emigrants because the population is small, receives fewer immigrants because it is hard to find: many emigrants from the larger patch simply return home. Again, our simple model cannot say anything about bifurcations away from the clustered state.

In some informal explorations of a two-dimensional nearest-neighbor system, we have observed "islands" of spatiotemporal periodicity, each of different phase, separated from one another by regions of aperiodic dynamics. We also observed temporally period-three solutions in which there was a tremendous variation in the actual values attained by the various oscillators, even though each was following a three-cycle. These are analogous to the odd-out-of-phase orbits described here.

ACKNOWLEDGMENTS

REFERENCES

Allen, J. C. 1975. Mathematical models of species interactions in time and space, *Am. Nat.* **109**, 319–342.

Allen, J. C., Schaffer, W. M., and Rosko, D. 1993. Chaos reduces species extinction by amplifying local population noise, *Nature (London)* **364**, 229–232.

Baier, G., and Klein, M. 1990. Maximum hyperchaos in generalized Hénon maps, *Phys. Lett. A* **151**, 281–284.

Baker, G. L., and Gollub, J. P. 1996. "Chaotic Dynamics: An Introduction," 2nd ed., Cambridge Univ. Press, Cambridge, UK.

Brown, J. H., and Kodric-Brown, A. 1977. Turnover rates in insular biogeography: Effect of immigration on extinction, *Ecology* **58**, 445–449.

Christiansen, E. 1983. Fluctuations in some small rodent population in Norway 1971–1979, *Holarctic Ecol.* **6**, 24–31.

Collet, P., and Eckmann, J.-P. 1980. "Iterated Maps on the Interval as Dynamical Systems," Birkhäuser, Basel.

Comins, H. N., and Hassell, M. P. 1996. Persistence of multispecies host–parasitoid interactions in spatially distributed models with local dispersal, *J. Theor. Biol.* **183**, 19–28.

Comins, H. N., Hassell, M. P., and May, R. M. 1992. The spatial dynamics of host–parasitoid systems, *J. Anim. Ecol.* **61**, 735–748.

Daido, H. 1984a. Coupling sensitivity of chaos, *Prog. Theor. Phys. Suppl.* **79**, 75–95.

Daido, H. 1984b. Coupling sensitivity of chaos, *Prog. Theor. Phys.* **72**, 853–856.

Day, J. R., and Possingham, H. P. 1995. A stochastic metapopulation model with variability in patch size and position, *Theor. Popul. Biol.* **48**, 333–360.

den Boer, P. J. 1981. On the survival of populations in a heterogeneous and variable environment, *Oecologia* **50**, 39–53.

Doebeli, M. 1995. Dispersal and dynamics, *Theor. Popul. Biol.* **47**, 82–106.

Eckmann, J.-P., and Ruelle, D. 1985. Ergodic theory of chaos and strange attractors, *Rev. Mod. Phys.* **57**, 617–656.

Ferretti, A., and Rahman, N. K. 1987a. Coupled logistic maps in physico-chemical processes: Coexisting attractors and their implications, *Chem. Phys. Lett.* **140**, 71–75.

Ferretti, A., and Rahmann, N. K. 1987b. A study of coupled logistic maps and their usefulness for modelling physico-chemical processes, *Chem. Phys. Lett.* **133**, 150–153.

Ferretti, A., and Rahman, N. K. 1988. A study of coupled logistic map and its applications in chemical physics, *Chem. Phys.* **119**, 275–288.

Frøyland, J. 1983. Some symmetric, two-dimensional, dissipative maps, *Physica D (Amsterdam)* **8**, 423–434.

Fujita, K. 1983. Systems analysis of an acarine predator-prey system. II: Interactions in discontinuous environment, *Res. Popul. Ecol.* **25**, 387–399.

Gilpin, M., and Hanski, I. 1991. "Metapopulation Dynamics: Empirical and Theoretical Investigations," Academic Press, London.

Grebogi, C., Ott, E., and Yorke, J. A. 1983. Crises, sudden changes in strange attractors, and transient chaos, *Physica D (Amsterdam)* **7**, 181–200.

Gurney, W. S. C., and Nisbet, R. M. 1978. Predator–prey fluctuations in patchy environments, *J. Anim. Ecol.* **47**, 85–102.

Gyllenberg, M., Söderbacka, G., and Ericsson, S. 1993. Does migration stabilize local population dynamics? Analysis of a discrete metapopulation model, *Math. Biosci.* **118**, 25–49.

Hanski, I., and Gilpin, M. E. 1997. "Metapopulation Biology: Ecology, Genetics, and Evolution," Academic Press, San Diego.

Hanski, I., and Woiwood, I. 1993. Spatial synchrony in the dynamics of moth and aphid populations, *J. Anim. Ecol.* **62**, 656–668.

Hassell, M. P., Comins, H. N., and May, R. M. 1991. Spatial structure and chaos in insect population dynamics, *Nature (London)* **353**, 255–258.

Hassell, M. P., Miramontes, O., Rohani, P., and May, R. M. 1995. Appropriate formulations for dispersal in spatially structured models: Comments on Bascompte & Solé, *J. Anim. Ecol.* **64**, 662–664.

Hastings, A. 1992. Age dependent dispersal is not a simple process: Density dependence, stability, and chaos, *Theor. Popul. Biol.* **41**, 388–400.

Hastings, A. 1993. Complex interactions between dispersal and dynamics: Lessons from coupled logistic equations, *Ecology* **74**, 1362–1372.

Heino, M., Kaitala, V., Ranta, E., and Lindström, J. 1997. Synchronous dynamics and rates of extinction in spatially structured populations, *Proc. Roy. Soc. London B* **264**, 481–486.

Hilborn, R. 1975. The effect of spatial heterogeneity on the persistence of predator–prey interactions, *Theor. Popul. Biol.* **8**, 346–355.

Hogg, T., and Huberman, B. A. 1984. Generic behavior of coupled oscillators, *Phys. Rev. A* **29**, 275–281.

Holt, R. D., and Hassell, M. P. 1993. Environmental heterogeneity and the stability of host-parasitoid interactions, *J. Anim. Ecol.* **62**, 89–100.

Holyoak, M., and Lawler, S. P. 1996. The role of dispersal in predator–prey metapopulation dynamics, *J. Anim. Ecol.* **65**, 640–652.

Huffaker, C. B. 1958. Experimental studies on predation: Dispersion factors and predator–prey oscillations, *Hilgardia* **27**, 343–383.

Iwasa, Y., and Roughgarden, J. 1986. Interspecific competition among metapopulations with space-limited subpopulations, *Theor. Popul. Biol.* **30**, 194–214.

Kaneko, K. 1983. Transition from torus to chaos accompanied by frequency lockings with symmetry breaking, *Prog. Theor. Phys.* **69**, 1427–1442.

Kaneko, K. 1985. Spatial period-doubling in open flow, *Phys. Lett. A* **111**, 321–325.

Kaneko, K. 1987. Pattern competition intermittency and selective flicker noise in spatiotemporal chaos, *Phys. Lett. A* **125**, 25–31.

Kaneko, K. 1989a. Chaotic but regular posi-nega switch among coded attractors by cluster-size variation, *Phys. Rev. Lett.* **63**, 219–223.

Kaneko, K. 1989b. Spatiotemporal chaos in one- and two-dimensional coupled map lattices, *Physica D (Amsterdam)* **37**, 60–82.

Kaneko, K. 1990. Supertransients, spatiotemporal intermittency and stability of fully developed spatiotemporal chaos, *Phys. Lett. A* **149**, 105–112.

Kaneko, K. 1993. The coupled map lattice: introduction, phenomenology, Lyapunov analysis, thermodynamics and applications, *in* "Theory and Applications of Coupled Map Lattices" (K. Kaneko, Ed.), pp. 1–49, Wiley, Chichester.

Kendall, B. E., Schaffer, W. M., and Tidd, C. W. 1993. Transient periodicity in chaos, *Phys. Lett. A* **177**, 13–20.

Kishimoto, K. 1990. Coexistence of any number of species in the Lotka–Volterra competitive system over two patches, *Theor. Popul. Biol.* **38**, 149–158.

Klein, M., and Baier, G. 1991. Hierarchies of dynamical systems, *in* "A Chaotic Hierarchy" (G. Baier, and M. Klein, Eds.), pp. 1–23, World Scientific, Singapore.

Kook, K., Ling, F. H., and Schmidt, G. 1991. Universal behavior of coupled nonlinear systems, *Phys. Rev. A* **43**, 2700–2708.

Levin, S. A. 1974. Dispersion and population interactions, *Am. Nat.* **108**, 207–228.

Lindström, J., Ranta, E., and Lindén, H. 1996. Large-scale synchrony in the dynamics of capercaillie, black grouse and hazel grouse populations in Finland, *Oikos* **76**, 221–227.

Lloyd, A. L. 1995. The coupled logistic map: A simple model for the effects of spatial heterogeneity on population dynamics, *J. Theor. Biol.* **173**, 217–230.

López-Ruiz, R., and Pérez-García, C. 1991. Dynamics of maps with a global multiplicative coupling, *Chaos Solitons Fractals* **1**, 511–528.

López-Ruiz, R., and Pérez-García, C. 1992. Dynamics of two logistic maps with a multiplicative coupling, *Int. J. Bifurcations Chaos* **2**, 421–425.

Losson, J., and Mackey, M. C. 1994. Coupling induced statistical cycling in two diffusively coupled maps, *Physica D (Amsterdam)* **72**, 324–342.

May, R. M. 1976. Simple mathematical models with very complicated dynamics, *Nature (London)* **261**, 459–467.

Myrberget, S. 1973. Geographical synchronism of cycles of small rodents in Norway, *Oikos* **24**, 220–224.

Nachman, G. 1981. Temporal and spatial dynamics of an acarine predator–prey system, *J. Anim. Ecol.* **50**, 435–451.

Nachman, G. 1976. Systems analysis of acarine predator–prey interactions. II. The role of spatial processes in system stability, *J. Anim. Ecol.* **56**, 267–281.

Nakamura, K., and Ohgushi, T. 1983. Studies on the population dynamics of a thistle-feeding lady beetle, *Henosepilachna pustulosa* (Kôno) in a cool temperate climax forest. III. The spatial dynamics and the analysis of dispersal behaviour, *Res. Popul. Ecol.* **25**, 1–19.

Nee, S., and May, R. M. 1992. Dynamics of metapopulations: Habitat destruction and competitive coexistence, *J. Anim. Ecol.* **61**, 37–40.

Pollard, E. 1991. Synchrony of population fluctuations: The dominant influence of widespread factors on local butterfly populations, *Oikos* **60**, 7–10.

Pomeau, Y., and Manneville, P. 1980. Intermittent transition to turbulence in dissipative dynamical systems, *Commun. Math. Phys.* **74**, 189–197.

Pulliam, H. R. 1988. Sources, sinks, and population regulation, *Am. Nat.* **132**, 652–661.

Pulliam, H. R. 1996. Sources and sinks: Empirical evidence and population consequences, *in* "Population Dynamics in Ecological Space and Time" (O. E. Rhodes, R. K. Chesser, and M. H. Smith, Eds.), pp. 45–69, Univ. of Chicago Press, Chicago.

Ranta, E., Kaitala, V., Lindström, J., and Lindén, H. 1995a. Synchrony in population dynamics, *Proc. Roy. Soc. London B* **262**, 113–118.

Ranta, E., Lindström, J., and Lindén, H. 1995b. Synchrony in tetraonid population dynamics, *J. Anim. Ecol.* **64**, 767–776.

Reeve, J. D. 1988. Environmental variability, migration, and persistence in host–parasitoid systems, *Am. Nat.* **132**, 810–836.

Rohani, P., May, R. M., and Hassell, M. P. 1996. Metapopulations and equilibrium stability: The effects of spatial structure, *J. Theor. Biol.* **181**, 97–109.

Rohani, P., and Miramontes, O. 1995. Host-parasitoid metapopulations: The consequences of parasitoid aggregation on spatial dynamics and searching efficiency, *Proc. Roy. Soc. London B* **260**, 335–342.

Rössler, O. E. 1979. An equation for hyperchaos, *Phys. Lett. A* **71**, 155–157.

Ruxton, G. D. 1996. Density-dependent migration and stability in a system of linked populations, *Bull. Math. Biol.* **58**, 643–660.

Ruxton, G. D., and Doebeli, M. 1996. Spatial self-organization and persistence of transients in a metapopulation model, *Proc. Roy. Soc. London B* **263**, 1153–1158.

Ruxton, G. D., and Rohani, P. 1996. The consequences of stochasticity for self-organized spatial dynamics, persistence and coexistence in spatially extended host-parasitoid communities, *Proc. Roy. Soc. London B* **263**, 625–631.

Sabelis, M. W., and Diekmann, O. 1988. Overall population stability despite local extinction: The stabilizing influence of prey dispersal from predator-invaded patches, *Theor. Pop. Biol.* **34**, 169–176.

Sakaguchi, H., and Tomita, K. 1987. Bifurcations of the coupled logistic map, *Prog. Theor. Phys.* **78**, 305–315.

Smith, C. H. 1983. Spatial trends in Canadian snowshoe hare, *Lepus americanus*, population cycles, *Can. Field-Naturalist* **97**, 151–160.

Sutcliffe, O. L., Thomas, C. D., and Moss, D. 1996. Spatial synchrony and asynchrony in butterfly population dynamics, *J. Anim. Ecol.* **65**, 85–95.

Thomson, J. M. T., and Stewart, H. B. 1986. "Nonlinear Dynamics and Chaos," Wiley, Chichester.

Van Buskirk, R., and Jeffries, C. 1985. Observation of chaotic dynamics of coupled nonlinear oscillators, *Phys. Rev. A* **31**, 3332–3357.

Waller, I., and Kapral, R. 1984. Spatial and temporal structure in systems of coupled nonlinear oscillators, *Phys. Rev. A* **30**, 2047–2055.

Wang, X., and Lowenstein, J. H. 1990. Scaling relations for thermodynamic functions of circle maps, *Phys. Rev. A* **41**, 5721–5724.

Wang, X., Maineri, R., and Lowenstein, J. H. 1989. Circle-map scaling in a two-dimensional setting, *Phys. Rev. A* **40**, 5382–5389.

Wiggins, S. 1988. "Global Bifurcations and Chaos: Analytical Methods," Springer-Verlag, New York.

Wiggins, S. 1990. "Introduction to Applied Nonlinear Dynamical Systems and Chaos," Springer-Verlag, New York.

Yamada, T., and Fujisaka, H. 1983. Stability theory of synchronized motion in coupled-oscillator systems. II. The mapping approach, *Prog. Theor. Phys.* **70**, 1240–1248.